DETERMINATION OF THE RELATIVE LINE STRENGTHS OF THE $A^2A' \leftarrow X^2A''$ AND (200)$\leftarrow$(000) TRANSITIONS OF HO_2

Thesis by

Fernando L. Rosario-Ortiz

In Partial Fulfillment of the Requirements for the Degree of

Master of Science

California Institute of Technology

Pasadena, California

2002

(Submitted September 28, 2001)

To those who believed in me...

Acknowledgments

The work presented in these pages represents for me the culmination of a period of my life and also, and most importantly, the most important achievement so far. But standing at this point I realize the tremendous amount of support that I have received from several people during my life and here is where I stop for a minute and say THANK YOU.

First of all I would like to thank my family, specially my mother Myriam, my two brothers Jorge (good luck with college) and Nydia (a new mom), and Lute, for all the support and faith. It is nice to know that no matter what I will still have all these people.

All my friends and colleagues back in Puerto Rico. Nadia Cordero for having introduced me to the fascinating world of chemistry, Edwin Quiñones whom I learned a lot from and who I still to this day consider to be an excellent advisor and friend, and Rafael Arce for teaching me that there is more to physical chemistry than quantum mechanics. To my good friends at the University of Puerto Rico; Carlos Crespo, Zuleika Cedeño, Jose Díaz, Carlos Conde, Angel Cruz, Angel Morales and many others; and also to my other puertorrican friends here in California, Luis Vazquez, Armando Rivera, Jose Rivera and Amy Brewster.

A big special thank you to my girlfriend Rebeca Gonzalez for supporting me and for being my best friend during the past nine months, maybe the toughest time in my life so far. I fell incredibly fortunate to have such a special person by my side giving me love and support.

To my advisors Mitchio Okumura and Stan Sander and to all my colleagues in Caltech and JPL, Lance, Claire, Eva, Julio, Andrei, Bill, Trevor, Dave and Sergei. All

my friends at Caltech, Shelley, Libby, Joe, Julie, Dave, Rachel and everyone else. A big special thanks for Dian Buchnes for having helped me throughout these past two years, especially this past few months.

And to all the people that I forgot to mention, thanks and you know who you are...

Fernando Rosario
September 18, 2001

Abstract

The hydroperoxyl radical (HO_2) has been one of the most studied triatomic radicals during the past few decades. Its roles in atmospheric chemistry through the HO_X cycle as well as in processes such as combustion have made the study of this radical extremely important. In the past three decades the interest in the spectroscopy of this molecule has increased due in part by the need of detecting this radical in several different environments. Although its UV, mid- and far-IR transitions have been studied extensively, its near-IR transitions have not received much attention until recently. Among the transitions observed in this region, the $A^2A' \leftarrow X^2A''$ first electronic transition and the (200)$\leftarrow$ (000) first OH overtone transition are two of the most important. These bands offer many advantages for detection of HO_2 in kinetic experiments and possibly in situ. Due to the importance of these two bands, information on their intensity is needed to measure accurately the concentration of HO_2. An apparatus has been constructed to measure the line strengths of the A$\leftarrow$X electronic transition at 1.43 μm and the (200)$\leftarrow$(000) first OH overtone transition at 1.51 μm by diode laser absorption spectroscopy.

Table of Contents

List of Figures

I. Introduction

The hydroperoxyl radical (HO_2) is one of the most studied tri-atomic radicals. This radical has important implications in many different areas, such as ozone depletion, combustion and oxidation processes. HO_2 and its other homologues (ROO• radicals) are important since they are the principal intermediates in the low temperature oxidation of organic materials.

However, despite the importance of this radical, it is difficult to measure low concentrations of it. Diverse spectroscopic studies have been performed on HO_2 examining the far-IR, [1,2] mid-IR, [3-5] and UV [5-7] regions in order to develop sensitive methods to monitor the low concentrations of this radical in the atmosphere and in laboratory studies. Historically, the most utilized methods have been direct absorption in the UV [8-11] and far-IR. [12,13] The UV is especially sensitive, but this method does have a drawback because several molecules interfere with its detection in these regions and also because the lack of structure of this transition.

Growing interest in the near-IR spectroscopy of HO_2 during the last twenty years has suggested that detection in this region may provide a way to probe this radical in the laboratory as well as in the atmosphere. There are two major HO_2 bands in this region, the $A^2A' \leftarrow X^2A''$ first electronic transition at 1.43 μm and the (200)←(000) first OH overtone at 1.51 μm. However, the lack of information on the intensities of these bands has limited the use of this region to monitor HO_2 concentration. Currently, only two HO_2 kinetic studies employing the near-IR absorption of HO_2 have been performed. [14,15] and

the number of line strength measurements and/or calculations for both of these transitions are not that numerous.

The aim of this work is to measure the relative line strengths for these two specific HO_2 transitions in the 1.51 and 1.43 microns regions. Information on these line strengths can be useful for monitoring HO_2 concentration in laboratory studies as well as in the altmosphere. The relative line strengths will be measured by diode laser spectroscopy. In order to measure the relative line strengths, a near-IR diode laser system has been build. The system that was constructed for these purposes includes the use of a multi-pass Herriott cell as well as two diode lasers and an InGas detector. The Herriott cell is needed in order to accomplish HO_2 detection due to its low concentration obtained from specific production methods.

Before going into the specifics of the apparatus, a brief background is presented in which the general spectroscopic characteristics of HO_2 are discussed. A brief review of line strengths and intensities is also presented. Details on the HO_2 chemical and spectroscopical simulations are also presented and discussed. Appendices 1-3 include the codes and information used to simulate the chemistry and spectroscopy of HO_2 as well as important information about the simulations.

II. Background Information

A. HO_2 Detection-A review

The spectroscopy of HO_2 has been studied extensively during the past few decades. [1-13] Due to its importance in many different combustion and atmospheric reactions, several spectroscopic techniques have been used to study its IR and UV

spectrum and to develop sensitive methods for monitoring its concentration. Detection of HO_2 has largely been based upon monitoring the $B^2A' \leftarrow X^2A''$ UV absorption. This is a strong transition, but unfortunately this transition is broad and unstructured. Experiments involving the $A^2A' \leftarrow X^2A''$ transition in the near-IR have shown that this transition in particular will be suitable for HO_2 monitoring. Another transition in this region, the (200)←(000) OH overtone also appears as a possibility for HO_2 detection.

B. HO_2 Structure and Spectroscopical Properties

The structure of HO_2 can easily be obtained from molecular orbital theory by adding a hydrogen atom to the oxygen molecule. The GVB molecular orbital diagram for the ground and the first two electronic states of HO_2 are presented below.

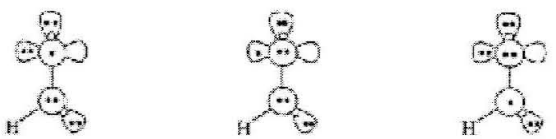

In 1952, Walsh [16] predicted that the ground state would have an A″ geometry which is strongly bent, and a A' first excited state which will be closer to linearity than the ground state. The B excited state was predicted also to have A" geometry by the same considerations. The A state is ~ .79 eV and the B state is ~5 eV above the ground state. These predictions were confirmed later by Gole et al.[17] and Buenker et al.[18] For the X^2A'' state, Osmann et al.[19] obtained the following equilibrium geometry: $r_{HO} = 0.97$ Å, $r_{OO} = 1.34$ Å and $\alpha = 103.11°$ where α refers to the angle between the O-H and the O-O bond.

HO_2 is classified as a near-prolate asymmetric top molecule with an asymmetry parameter b (defined below) of approximately -10^{-3}.

$$b = \frac{C - B}{2(A - D)}$$

In this expression, A, B and C are the rotational constants for the near-prolate asymmetric top molecule and D = 1/2(B+C). These constants are resented in Table 1.

For an asymmetric top molecule like HO_2, the rotational constants A, B and C are different and therefore the Hamiltonian and the energy will be functions of these constants. The HO_2 free radical is classified as a near-prolate asymmetric top. It is a prototypical light and unsymmetrical triatomic molecule with rotational constants A, B and C equal to ~20, 1 and 1 in cm^{-1}. The rotational constants for the ground and first electronic state are given in table 1.

Table 1. Spectroscopic constants for HO_2

Constant	A^2A' (cm^{-1})	X^2A'' (200) (cm^{-1})	X^2A'' (000) (cm^{-1})
A	20.47169	18.2120	20.34244
B	1.020635	1.1170	1.02
C	0.967336	1.0566	1.055591
Δ_N	4.13×10^{-6}	5.2×10^{-6}	3.87×10^{-6}
Δ_{NK}	0.000139	0.00012	0.000115
Δ_K	0.004866	0.0032	0.004119
δ_N	2.33×10^{-7}	n/a	2.05×10^{-7}
δ_{NK}	9.42×10^{-5}	n/a	6.59×10^{-5}
ν_0	7030	6649	6649

The energy levels of a near-prolate top molecule falls between that of a prolate and of an oblate molecule so it is convenient to introduce a notation for this. For this kind of molecule the levels are labeled N_{KaKc}, where N is a good quantum number, but K_a and K_c become good quantum numbers only in the prolate or oblate top limits. In this

notation, the sum of K_a and K_c is N or N+1.For these rotational levels the energy is given by the same expression used for the energy levels of a symmetric top molecule plus additional terms introduced by slight molecular asymmetry as described in the following equation:

$$F(N,K) = \bar{B}N(N+1) + \left(A - \bar{B}\right)\left[1 - \frac{3b^2}{8}\right]K^2 + \Delta B^K{}_{eff}\, N(N+1)$$
$$+ \Delta D^K{}_{eff}\, N^2(N+1)^2 - D_K K^4 - D_{NK} N(N+1)K^2 - D_N N^2(N+1)^2$$

where $\bar{B}$ = *1/2(B+C)* and D_K, D_{NK} and D_N are the three centrifugal distortion constants for a non-rigid symmetric top. In this expression *b* is the asymmetry parameter. For HO_2 this parameter has a value of ~10^{-3}. Because of the very low degree of asymmetry of HO_2, it is possible to assume that K, the component of the total angular momentum N along the near-prolate top axis, is a good quantum number. $\Delta B^K{}_{eff}$ and $\Delta D^K{}_{eff}$ are functions of *b* and *K*. [14] These values are zero for *K*>2. Note that by definition the coefficient of K^2 is greater than zero so that for a given value of N, the K levels increase in energy.

For asymmetric top molecules like HO_2 the selection rules are more complicated that those for a symmetric top molecule. Apart from the ΔJ= -1, 0, 1 one has another set of rules. They will be dependent on each non-vanishing dipole moment component of the molecule. In general one can express the dipole moment of a molecule in terms of its projections along the molecular a, b and c axis, these axis defined by the moments of inertia of the molecule, based on the requirement that $I_a \leq I_b \leq I_c$. A transition is classified as an a-type if $\mu_a \neq 0$ and $\mu_b = \mu_c = 0$, where μ_X (X=a, b or c) is the projection of μ in the molecular a, b and c axis system. For this type of transition $\Delta K_a = 0$ (±2, ±4,…) and ΔK_c

= 1 (±3, ±5,...). If $\mu_b \neq 0$ then the transition is classified as an b-type and only transition with the selection rules $\Delta K_a = 1$ (±3, ±3,...) and $\Delta K_c = 1$ (±3, ±5,...) will be allowed. For a transition to be classified as an c-type transition, $\mu_c \neq 0$ and then transitions with the selection rules $\Delta K_a = 1$ (±3, ±3,...) and $\Delta K_c = 0$ (±2, ±4,...) are allowed.

C. HO_2 Spectroscopy

The first electronic spectrum observed for the HO_2 radical was a broad absorption band between 185 and 280 nm. This band, later assigned to the second electronic (B) state, showed no structure indicating the repulsive character of this state. Later investigations of the near-IR region [20,21] showed the existence of bands centered at 1.43 and 1.51 microns, latter assigned to the first electronic (A) and to the first OH overtone transitions of the ground state.

Hunziker and Wendt [22] observed the near infrared absorption spectrum of HO_2 in the gas phase between 0.5 and 2.2 μm. The observed bands and assignments for HO_2 and DO_2 are presented in Table 2.

Table 2. Band Assignment for HO_2 and DO_2 in the near-IR

HO_2 Spectrum (μm)	Type	DO_2 Spectrum (μm)	Type	Assignment
1.504±.0.001	||	2.022±0.003	||	$^2A''(200) \leftarrow {}^2A''(000)$
1.425±0.002	⊥	1.425±0.002	⊥	$^2A'(000) \leftarrow {}^2A''(000)$
1.255±0.002	⊥	1.254±0.002	⊥	$^2A'(001) \leftarrow {}^2A''(000)$

The 1.43 μm band shows a ⊥-type structure with a number of distinct sub-bands with an average separation of 44 cm^{-1}. [22] The 1.50 μm absorption band, with a parallel-type structure, shows a P, R branch separation of approx. 42 cm^{-1}. The || -type band at 1.50 microns was assigned to the O-H and O-D overtone vibration in the ground state.

For this transition, the anharmonicity constants were estimated as x_{11}^{0} = -86±5 for HO_2 and -54±7 cm^{-1} for DO_2.

The main electronic band of HO_2 (at 1.43 μm) is a c-type transition with non-zero transition dipole moment perpendicular to the plane of the molecule. The general selection rules for such transitions are $\Delta K_a = \pm 1$ and $\Delta K_c = 0$ for a molecule like HO_2. [23]

In their high-resolution study, Fink and Ramsay [24] confirmed that this band corresponded to a transition from the ground state to the first electronic state and that this state was the only stable electronic state for the molecule. Further analysis of the rotational structure of this electronic transition was performed by Freedman and Jones [25] and later by Tuckett and co-workers. [28] Recent high-resolution studies of the 1.43 band [14] have provided a complete assignment of the emission lines of HO_2 in this region, as well as accurate rotational parameters.

The OH stretching vibrational overtone is restricted to the plane of the molecule and generates an alternating dipole with components along the a and b inertial axis. [26] The overtone band of the HO_2 radical is an a/b Hybrid (parallel), the a-type having ΔK_a = 0 and the b-type $\Delta K_b = \pm 1$. The predominant emission reported by Tuckett et al. [23], is the ΔK_a=0 a-type. Simulations of the electronic and overtone transitions are shown in Figures 1 and 2.

D. HO_2 Forbidden Bands

One of the most important conclusions obtained from the analysis of the structure of the 1.43 μm band was the observation and confirmation of the existence of $\Delta K_a = 0$ sub-bands which are forbidden for c-type transitions. [23,24] Some of the lines in the 7035-

7044 cm^{-1} regime ($\Delta K_a = 0$) were found to obey the selection rules $\Delta K_a = 0$, $\Delta K_c = \pm 1$. These selection rules correspond to an a-type transition, which must be magnetic dipole in character. Tuckett et al. [23] suggested that these transitions resulted from the Renner interaction. Fink et al. [24] in their reinvestigation of the $A^2A' \rightarrow X^2A''$ transition at high resolution found that many of the forbidden transitions must be interpreted as magnetic dipole transitions since they connect rovibronic states of the same parity.

Magnetic dipole transitions are typically ~10^5 times weaker than allowed electric dipole transitions, but because they obey different selection rules, they may give rise to spectral lines where electric dipole transitions are forbidden. Electric dipole transitions connect states of opposite parities (ΔK_c = even). Magnetic dipole transitions connect states of the same parity (ΔK_c = odd). For HO_2, electric and magnetic dipole lines will coincide except when K_a = 1,2. These types of transitions are normally too weak to be observed among electric-dipole transitions, but HO_2 is a favorable case since the electric dipole transition moment for the electronic transition is very small. For example, at the X state equilibrium geometry, the electric dipole moment can have a value of ~0.017 D and the magnetic dipole of ~0.0089 D (in the z-axis), giving then a ratio of intensities of ~0.27, making the detection of magnetic dipole transitions possible. In their theoretical work, Osmann et al. [2] confirmed the importance of both magnetic dipole transition moment and Renner effect for making forbidden $\Delta K_a = 0$ transitions visible. Some of the ΔK_a=0 transitions were attributed to magnetic dipole and others were attributed to electric dipole transitions that arise from the Renner effect.

Although these transitions have been studied, only theoretical calculations for the line strength of the electronic transition and a few measurements on the overtone line strengths have been performed.

E. Line strengths-A theoretical approach

Line strengths for electric dipole transitions are related to the integrated absorption coefficient by

$$I(f \leftarrow i) = \int \varepsilon(\nu) d(\nu) = \frac{8\pi^3 N_A \nu_{if} \exp(-E''/kT)(1-\exp(-hc\nu_{if}/kT))}{(4\pi\varepsilon_0)3hcQ} S(f \leftarrow i)$$

where $\varepsilon(\nu)$ is the absorption coefficient and ν_{if} = (E' - E")/hc. For magnetic dipole transitions, a similar expression applies in which the c in the denominator is replaced by c^3 and d_A is used instead of μ_A in the S expression (see below). The partition function Q is given by

$$Q = \sum_w g_w \exp(-E_w/kT)$$

in which w and E_w are the degeneracy and energy of the w state. The expression for the line strength, S, is defined as

$$S(f \leftarrow i) = \sum_{\Phi'_{INT}\Phi''_{INT}} \sum_{A=XYZ} \left| \langle \Phi'_{INT} | \mu_A | \Phi''_{INT} \rangle \right|^2$$

where Φ'_{INT} and Φ''_{INT} are eigenfunctions of the molecular Hamiltonian corresponding to the eigenvalues E' and E" respectively. In the case of degeneracies, the line strength is obtained by adding the individual transition probabilities for all transitions between the degenerate states. The μ_A term refers to the component of the molecular dipole moment

along the A axis (A= X, Y, Z), with this axis having the origin at the molecular center of mass.

The matrix elements in the line strength expression can be written in terms of separable wavefunctions as

$$\left\langle \Phi'_{nspin}\, \Phi'_{rot}\, \Phi'_{vib}\, \Phi'_{elect} \left| \mu_s^{(1,\pm 1)} \right| \Phi''_{nspin}\, \Phi''_{rot}\, \Phi''_{vib}\, \Phi''_{elect} \right\rangle$$

in which μ is obtained by changing the axis system to the nuclear-center system (ξ, η, ς).

$$\mu_S^{(1,\pm 1)} = \frac{\left| \mp \mu_\xi + i\mu_\eta \right|}{\sqrt{2}}; \mu_S^{(1,0)} = \mu_\varsigma$$

where μ_ξ, $\mu_\eta$and μ_ζ are the μ components in this new axis system. This axis system change is appropriate for setting up the rovibronic wave equation in the Born-Oppenheimer approximation.

The dipole moment operator is independent of nuclear spin coordinates so it can be factored out from the wavefunction expression. The rotational and vibrational parts can also be separated and the rotational wavefunctions can be expanded as a linear combination of asymmetric top wavefunctions as

$$\Phi'_{ROT} = \sum_{k'=-N'}^{N'} c_{k'}^{(N')} \left| N', k', m' \right\rangle$$

with a similar expression for Φ''_{Rot}.

With the use of analytical expressions for the rotational wavefunctions and a subsequent separation of electronic and vibrational coordinates, a final expression for the line strength factor is obtained:

$$S(f \leftarrow i) = g_{ns}(2S+1)(2N''+1)(2N'+1) \times \left| \sum_{k'=-N'}^{N'} \sum_{k'=-N''}^{N''} c_{k'}^{(N')*} c_{k''}^{(N'')} (-1)^{k'} \right.$$

$$\left. \times \sum_{\sigma=-1}^{1} \left\langle \Phi'_{vib} \left| \mu_m^{(1,\sigma)}(e', e'') \right| \Phi''_{vib} \right\rangle \begin{pmatrix} N'' & 1 & N' \\ k'' & \sigma' & -k' \end{pmatrix} \right|^2$$

The determination of the intensity of an overtone transition does not require the examination of electronic wavefunctions, therefore the intensity will be dependent only on the the rotational and vibrational wavefunctions. A simple expression for the intensity of an overtone transition, only including vibrational terms, can be obtained by expanding the expressions for the dipole moment and taking the non-linear terms. The expectaion value of these terms will give the expression for the transition dipole moment and therefore the intensity.

F. Previous results-Line strength measurements

Johnson and co-workers [27] measured the line center cross sections for the strongest absorption lines in the (200)←(000) overtone. From this study an integrated line strength value of ~1 x 10^{-20} cm^2 $molecule^{-1}$ cm^{-1} for the strongest line at 1.5090 μm was obtained. Taatjes and OH [14] measured the line strength for the 1.5093 μm line and obtained a value of 2.4 x 10^{-21} cm^2 molecule cm^{-1}. Osmann and co-workers [19] calculated line strengths and positions for several electric and magnetic dipole transitions in the 1.43 μm electronic band as a way of confirming the results of high-resolution studies by Fink and Ramsay. [24] In the later study, line strength measurements were not carried out. Similar calculations have not been made for the overtone, for which intensity measurements were performed for only a few lines by Oh. [14] Table 3 presents some cross sections values.

Table 3. Absorption cross sections for the HO_2 overtone transition [26]

λnm)	10^{20} σ, cm^2 $molecule^{-1}$
1.5082	6.2
1.5083	3.2
1.5086	3.4

1.5088	5.3
1.5090	4.5
1.5097	2.3

For the electronic and magnetic transitions, Osmann *et al.* [19] calculated intensities for the most intense allowed electronic transitions and for the most intense magnetic dipole transitions. Tables 4 and 5 present some results.

Table 4. Electric dipole transitions for the A-X emission band of HO_2 [19]

ν (cm^{-1})	I ($J\ mol^{-1}\ s^{-1}$)
7003.31	12320
7005.37	15390
7007.41	11200
7010.37	8246
7035.45	13010
7048.09	8006

Table 5. Magnetic dipole transitions for the A-X emission band of HO_2 [19]

ν (cm^{-1})	I ($J\ mol^{-1}\ s^{-1}$)
6999.02	2359
7000.63	2176
7007.32	1980
7010.97	2091
7039.43	1971

III. Experimental Section

A. HO_2 Spectroscopical Simulations

Simulations of the $A^2A' \leftarrow X^2A''$ first electronic transition and of the (200)←(000) first OH overtone transition were performed using the program Asyrot. Table 1 shows the rotational constants as well as the band origins for both transitions obtained from references (23) and (24).

1. (200)← (000) Transition Simulation

The (200)←(000) OH overtone transition was treated as an a/b hybrid transition, with the transition occurring in the plane of the molecule. [23, 26] The actual ratio of a:b is unknown but Tuckett and co-workers [23] reported the a band to be higher in intensity. For the simulation a ratio of 0.4 was used. Appendix 2 shows a typical output of the simulation in which only transitions with relatively high intensities are shown. The output shows the calculated frequency of the transition in vacuum wavenumbers as well as the type of transition, the corresponding assignment and Boltzmann intensities. For the a-type transition $\Delta K_a = 0$ and we therefore see a progression of P, Q and R branches corresponding to every $\Delta K_a = 0$, being the most intense ones the 0←0 and 1←1 transitions. For the b-type transition we have the most intense bands being the 1←0 and the 0←1. Figure 2 shows the combination of the two types of band with an approximated ratio of intensities of 0.40 (b/a).

2. $A^2A' \leftarrow X^2A''$ Transition Simulation

The $A^2A' \leftarrow X^2A''$ electronic transition is a c-type transition with the transition dipole perpendicular to the plane of the molecule. Figure 1 shows the simulation of this transition and Appendix 3 shows an output from this simulation. The main bands around the 7050 cm^{-1} region correspond to the ($K_a'' \leftarrow K_a'$) 1←0 and 0←1 transitions, each of them with its corresponding P, Q and R branches. The spectrum can be roughly divided into two regions with different K_a selection rules. The lines observed at wavenumbers higher than ~7050 cm^{-1} correspond to the $\Delta K_a = +1$ and the region below 7050 cm^{-1} correspond to $\Delta K_a = -1$. Each possible ΔK_a sub-band includes its own set of P, Q and R branches. The program used for these simulations does not include the spin-rotation

splitting due to the fact that HO_2 is a doublet radical. Each line in the simulation should be split into two J values, J = N-1/2 and J = N+1/2. This simulation does not include any forbidden transition, which exist in the experimental spectrum. [24] The intensities obtain from this simulations are obtained from simple Boltzmann distributions and rotational line strengths and in no manner represent experimental measurements and/or calculated intensities.

Due to the limited range of frequencies obtained from diode lasers, only relatively small regions of each band are examined. The spectral ranges of the diode lasers to be used are approximately ± 6 cm^{-1} from the center frequency of the laser. The diode lasers have center frequencies of 6622.5 and 6993.0 cm^{-1}, which limit the number of lines to be studied. Figures 3 and 4 shows the regions of each transition to be examined.

B. HO_2 Chemistry Simulations

Production of HO_2 is accomplished by ozone photolysis in a $H_2/O_2/N_2$ mixture. The ozone was obtained from an ozoniser which produced a mixture of ~1% ozone/oxygen at an applied power of 20 W. The 254 nm UV photolysis of ozone produces $O(^1D)$ with a yield of 0.85-0.90. [28] This atom is extremely reactive and reacts almost immediately with hydrogen to extract an H-atom. The remaining H-atom reacts with O_2 producing HO_2. The chemistry for this process was simulated using the FACSIMILE program. Appendix 1 shows the input used for the simulation, including all the reactions used and rate values at 298 K, as well as the concentration profile of several species for the first 100 ms.

The production of HO_2 was simulated using an initial rate for the dissociation of ozone of ~0.3 s^{-1} based on the UV flux at 254 nm obtained from the lamps (see below) and the cross section and dissociation quantum yield for ozone obtained from reference (28). The UV light is obtained from 16 mercury lamps (253.8 nm) arranged to give an estimated 0.3 s^{-1} for the photolysis rate of ozone. A plot of intensity of light vs. distance from the surface of the lamp is shown in figure 7. The UV flux for a system consisting of 16 lamps should be around 9 mW/cm^2. The lamps were located at a distance of ~7 cm from the surface of the cell and at an approx. distance of ~10 cm from the center of the cell. Please refer to figure 16 for details on the arrangement of the lamps.

Simulations performed showed that a concentration of ~10^{13} molecules/cc of HO_2 will be obtained by using the following initial conditions: $[O_3]_0=3.0x10^{16}$ molecules per cm^3 , $[O_2]_0=8.0x10^{17}$ molecules per cm^3 , $[H_2]_0=3.0x10^{17}$ molecules per cm^3 , $[N_2]_0=1x10^{18}$ molecules per cm^3. The simulation included the major mechanisms for HO_2 loss including self-reaction and wall reactions. Plots of the concentration of HO_2 and O_3 as a function of time are shown in figures 5 and 6.

The rate HO_2 formation is in the order of 10^{15} molecules cm^{-3} s^{-1} with a similar, but higher, rate of destruction. The highest HO_2 concentration (of ~ 10^{13} molecules cm^{-3}) is achieved at short times with an increase in the disappearance rate of HO_2 once HO_2 self-reaction and other HO_2-consuming reactions start to compete.

C. Development of the apparatus

Figure 8 shows a schematic of the experimental setup. The details will be discussed in the next paragraphs.

1. Flow system

As mentioned before, the gases needed in order to produce HO_2 are O_3, O_2, H_2 and N_2. An O_3/O_2 mixture is obtained from the ozoniser. The ratio of the mixture is approx. 1 % O_3/O_2 as determined by measuring the ozone concentration as a function oxygen pressure. Hydrogen and nitrogen flows are measured with Hastings Flowmeters. Calibration curves for the different flowmeters used can be found in figures 9-11. Calibrations were performed using a bubble flowmeter from Hastings. The gases were mixed and directed into the cell.

The vacuum system consisted of a 5.6 CFM vacuum pump connected to the system using 3" diameter PVC. The pressure inside the cell was measured using a 1000 torr baratron. The baratron read the pressure with an uncertainty of <100 mtorr. For a complete description see the calibration information for the 1000 torr head please refer to figures 12-13.

2. UV (254 nm) Mercury Lamp System

The *J* value required to obtain the necessary concentration was obtained from the simulation. See above. Sixteen UV (253.8 nm) lamps were purchased from UV Products. A plot of intensity of light vs. radial distance from the surface of the lamp is shown in figure 7.

The lamps were located at a distance of ~7 cm from the surface of the cell and at an approx. distance of ~10 cm from the center of the cell. The arrangement of the lamps is such that the whole cell will receive equal UV flux. Figure 16 shows the arrangement of the lamps.

3. Diode Lasers and Detection System

As explained in the introduction, the wavelengths needed for this experiment are 1.43 and 1.51 microns. For the first part of the experiment the 1.51 microns transition will be examined. The laser produces a cw pulse centered at 1510 nm with a FWHM of 0.2 nm. The detector is an InGaAs detector. The detector is sensitive to wavelengths from the UV to the near-IR range.

Temperature and current response for the 1510 nm laser was obtained by analyzing the fringes patterns of an etalon. A current response of ~0.04 cm^{-1}/mA and a temperature response of ~0.5 cm^{-1}/K was found, giving the diode an estimated range of ± 6 cm^{-1} from the central frequency.

4 Multipass (Herriott) Cell

A Herriott cell is used in order to increase the sensitivity. The theory behind Herriott cell has been discussed previously [29,30] and therefore only a brief discussion is given here. Two mirrors will confine the laser beam inside the cell for a finite time, giving rise to a large number of passes, which enhance the path length. Schematics of the mirror mounts (as design by Lance Christensen) are shown in figure 14. In our case the predicted path length will be around 30 times the separation of the mirrors. The number of reflections (r) can be approximated by the following expression, which will be a function of the mirror focal length and of the inter-mirror separation;

$$r = \frac{180}{180 - \cos^{-1}(2g^2 - 1)}$$

where g = 1 - d/R and d is the inter-mirror separation and R is the focal length. A plot of the number of spots vs mirror separation can be found in figure 15. In our current set-up, the number of reflection equals ~ 15 to give a total path length of ~1.6 m.

IV. Objectives

The relative line strengths for some of the rovibrational lines in the electronic ($A^2A' \leftarrow X^2A''$) transition as well as in the OH first overtone (200←000) transition are to be measured in this experiment. At this point, we cannot accurately determine the HO_2 concentration; instead the relative intensity of two lines will be measured.

A Voigt function will be used to fit the absorption profiles and subsequently will give the integrated absorption coefficient of one line relative to another. The Voigt function is a convolution of the pressure broadened Lorentzian with the Gaussian Doppler line shape. Under the experimental conditions a pressure of approximately 50 torr will be used so that pressure broadening should not be a major problem.

V. Results

The experimental set-up as well as the laser and detection system has been tested by examining the 1.51 μm lines of the H_2O molecule. The laser was also calibrated for its frequency response as a function of temperature and current. For the temperature, the frequency response was found to be ~ -0.4 cm^{-1}/ °C and for the current a value of 0.035 cm^{-1}/mA was found. These values were found by examining the fringe pattern of an etalon with the 1510 nm laser. For the temperature frequency response, the laser current was fixed and the temperature was varied while for the current frequency response the temperature was fixed.

Even thought the temperature and frequency response of the laser has been examined (by means of the change of frequency by changing either the current or temperature), the absolute values of frequency at a given current and temperature hasn't been determined yet. Complementary studies of the water lines in the 1.51 microns region will have to be performed in order to accomplish that.

VI. Conclusions

An apparatus has been constructed to measure the relative intensities of the first overtone and the first electronic transition of HO_2 are measured in this experiment by diode laser absorption spectroscopy. HO_2 production is accomplished by irradiating a mixture of O_3, O_2, H_2 and N_2 with UV light (253.8 nm) from mercury lamps. An increase in sensitivity is achieved by the use of a Herriott cell, which gives an estimated 1600 cm of pathlength.

VII. Bibliography

1) H. E. Radford, K. M. Evenson and C. J. Howard, J. Chem. Phys., 60, 3178 (1974)

2) K. V. Chance, K. Park, K. M. Evenson, L. R. Zink and F. Stroh, E. H. Fink and D. A. Ramsay, J. Mol. Spectrosc., 183, 418 (1997)

3) D. E. Milligan and M. E. Jacox, J. Chem. Phys., 38, 2627 (1963);J. Mol. Spectrosc., 42, 495 (1972), J. Mol. Spectrosc., 172, 407 (1995)

4) J. F. Ogilvie, Spectrochim. Acta 23A, 737 (1967); Nature 243, 210 (1973)

5) T. T. Paukert and H. S. Johnson, J. Chem. Phys., 56,2824 (1972)

6) H. Kijewski and J. Troe, Int. J. Chem. Kinet., 3, 223 (1971)

7) C. J. Hochanadel, J. A. Ghormley and P. J. Ogren, J. Chem. Phys., 56, 4426 (1972)

8) V. Catoire, R. Lesclaux and T. J. Wallinton, J. Phys. Chem., 100, 34, 14356 (1996)

9) S. L. Nickolaisen, C. M. Roehl and S. P. Sander, J. Phys. Chem. A., 104, 2, 308 (2000)

10) M. J. Kurylo and P. A. Ouellette, J. Phys. Chem., 91, 12, 3365 (1987)

11) S. P. Sander and M. E. Peterson, J. Phys. Chem., 88, 8, 1566 (1984)

12) J. M. Cronkhite, R. E. Stickel, J. M. Nicovich and P. H. Wire, J. Phys. Chem. A, 103, 3228 (1999)

13) M. A. Crawford, T. J. Wallinton and J. S. Francisco, J. Phys. Chem. A., 103, 3, 365 (1999)

14) C. A. Taatjes and D. B. Oh, Appl. Opt., 36, 24, 5817 (1997)

15) L. E. Christensen, B. Laszlo, C. H. Miller, J. J. Sloan, M. Okumura and S. P. Sander, unpublished results

16) A. D. Walsh, J. Chem. Soc. 65, 229, (1953)

17) J. C. Gole and E. F. Hayes, J. Chem. Phys., 57 360 (1972)

18) R. J. Buenker and S. D. Peryerimhoff, Chem. Phys. 28, 299 (1978)

19) G. Osmann, P. R. Bunker, P. Jensen, R. J. Buenker, J. Gu and G. Hirsch, J. Mol. Spectrosc., 197, 262 (1999)

20) H. E. Hunziker and H. R. Wendt, J. Chem. Phys., 64, 3488 (1976)

21) K. H. Becker, E. H. Fink, P. Langen and U. Schurath, J. Chem. Phys., 60, 4623 (1974)

22) H. E. Hunziker and H. R. Wendt, J. Chem. Phys., 60, 11 4622 (1974)

23) R. P. Tuckett, P. A. Freedman and W. J. Jones, Mol. Phys., 37, 2, 379 (1979)

24) E. H. Fink and D. A. Ramsay, J. Mol. Spectrosc., 185, 304 (1997)

25) P. A. Freedman and W. J. Jones, J. Chem. Soc. Faraday Trans. 2, 76, 207 (1976)

26) The plane of the molecule contains the *a* and *b* inertial axis, with the *c* axis perpendicular to the plane of the molecule.

27) T. J. Johnson, F. G. Wienhold, G. W. Harris and H. Burkhard, J. Phys. Chem., 95, 6499 (1991)

28) W. G. DeMore, S. P. Sander, D. M. Golden, R. F. Hampson, M. J. Kurylo, C. J. Howard, A. R. Ravishankara, C. E. Kolb and M. J. Molina, Chemical Kinetics and Photochemical Data for Use in Stratospheric Modeling, Evaluation No. 12, JPL Publication 97-4, Jet Propulsion Laboratory, Pasadena, CA

29) D. Herriott, H. Kogelnik and R. Kompfner, Appl. Opt., 3, 4, 523 (1964)

30) D. Herriott and H. J. Schutle, Appl. Opt., 4, 8, 883 (1965)

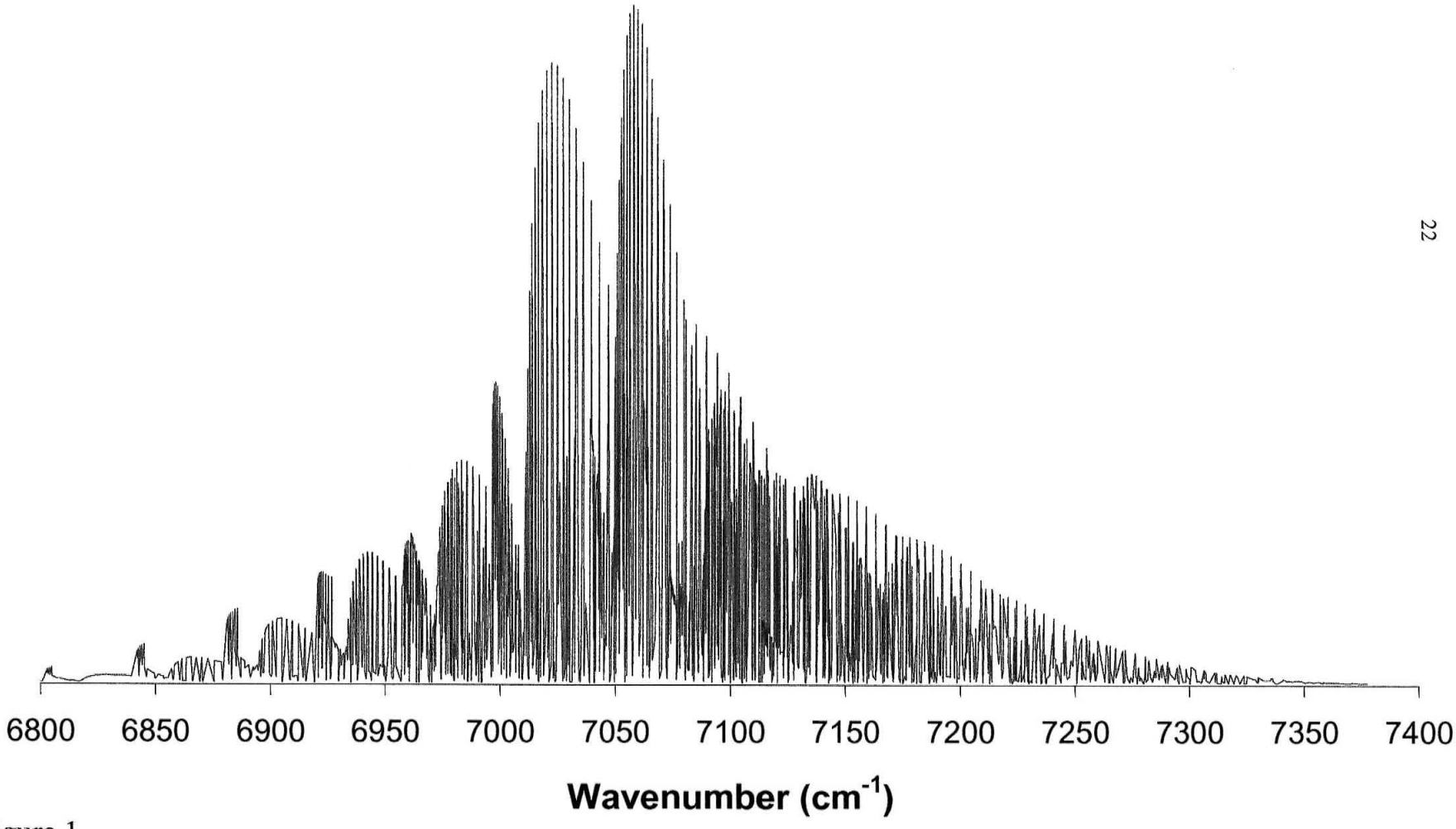
HO2 Electronic Transition
6800
6850
6900
6950
7000
7050
7100
7150
7200
7250
7300
7350
7400
Wavenumber (cm-1)

Figure 1

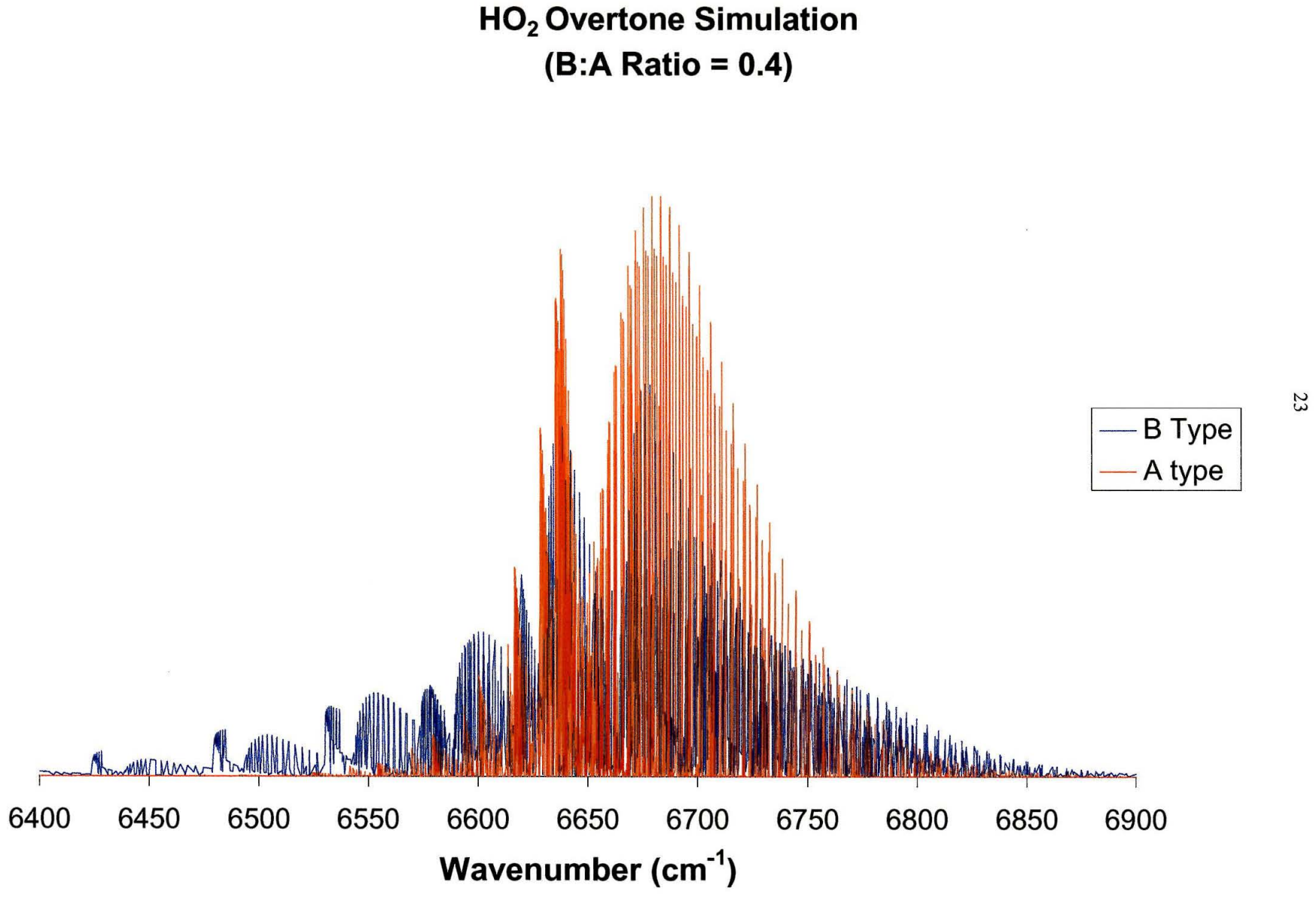
HO2 Overtone Simulation
(B:A Ratio = 0.4)
B Type
A type
6400
6450
6500
6550
6600
6650
6700
6750
6800
6850
6900
Wavenumber (cm-1)

Figure 2

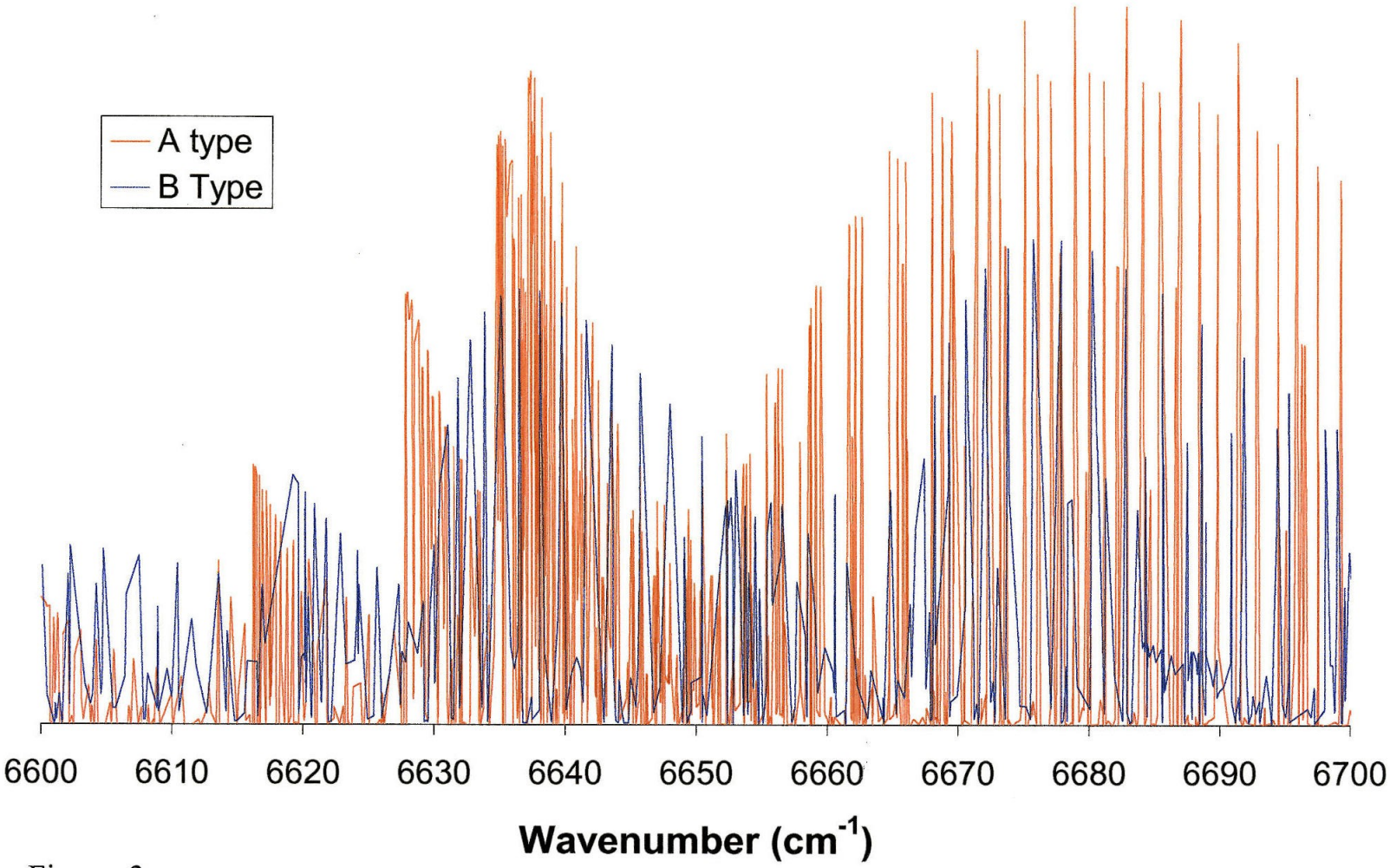
HO2 Overtone Simulation
(B:A Ratio = 0.4)
A type
B Type
6600
6610
6620
6630
6640
6650
6660
6670
6680
6690
6700
Wavenumber (cm-1)

Figure 3

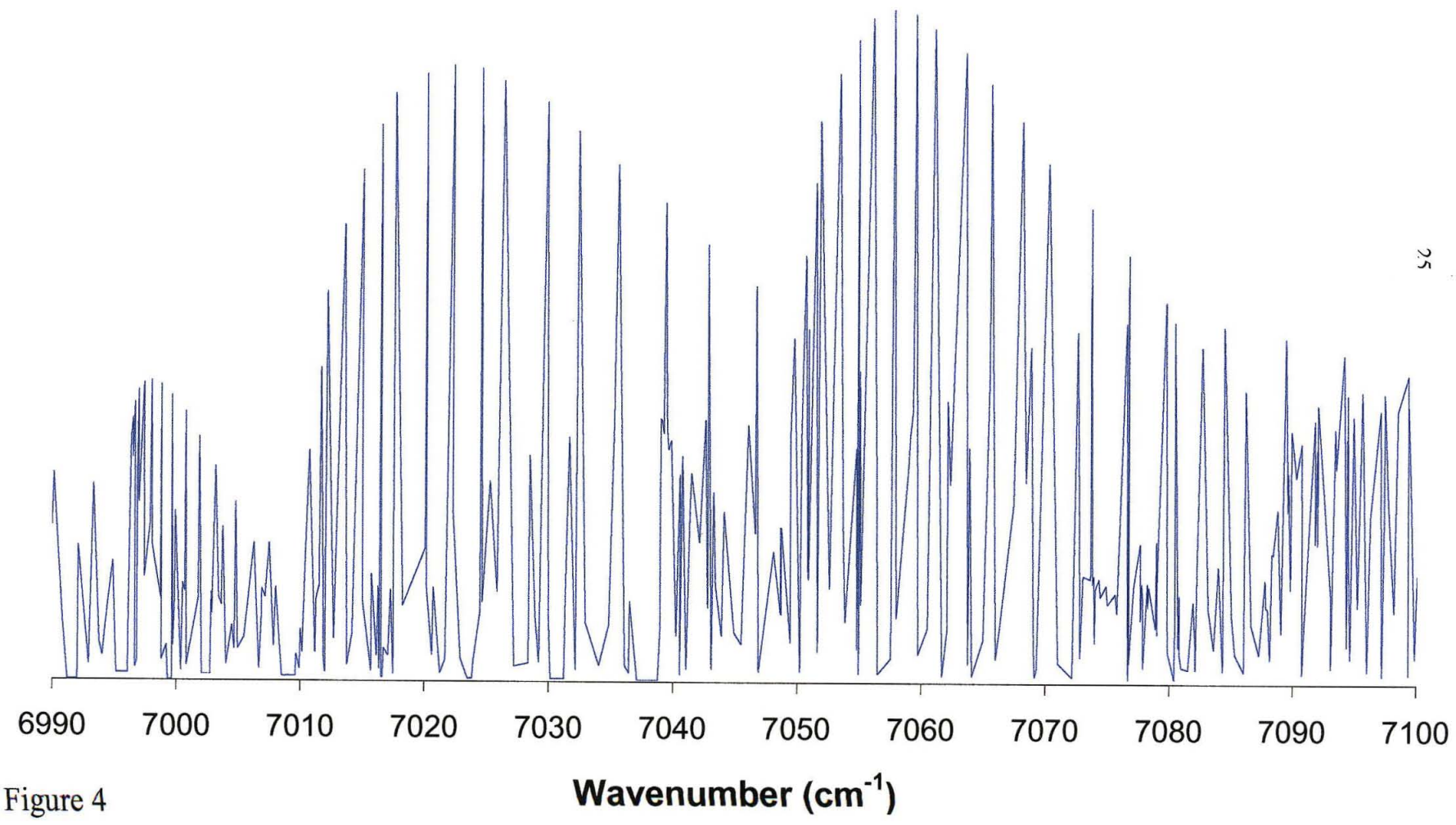
HO2 Electronic Transition
6990
7000
7010
7020
7030
7040
7050
7060
7070
7080
7090
7100
Wavenumber (cm-1)

Figure 4

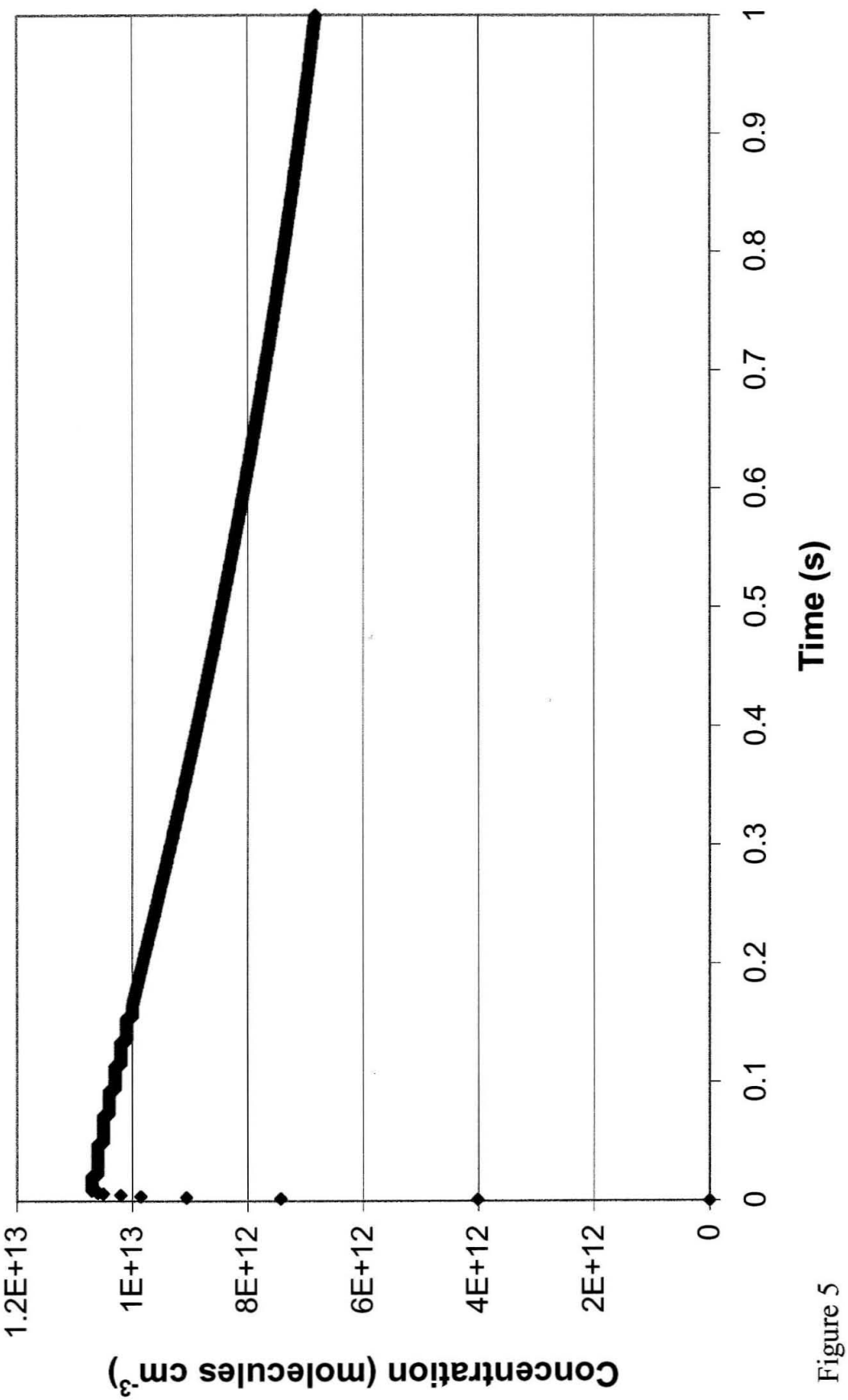
HO2 Concentration Profile
Concentration (molecules cm-3)
1.2E+13
1E+13
8E+12
6E+12
4E+12
2E+12
0
0
0.1
0.2
0.3
0.4
0.5
0.6
0.7
0.8
0.9
1
Time (s)

Figure 5

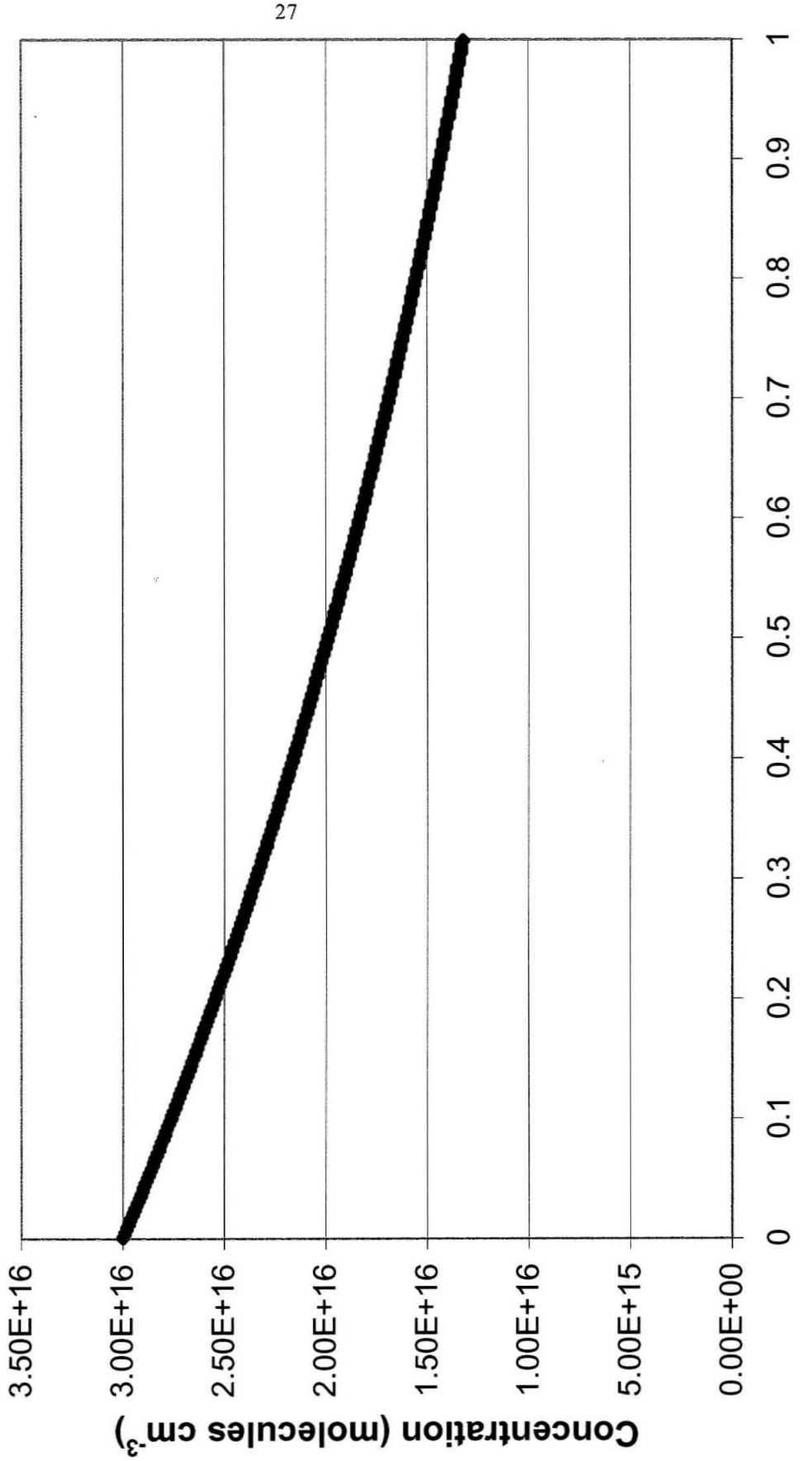
O_3 Concentration Profile
Concentration (molecules cm^{-3})
3.50E+16
3.00E+16
2.50E+16
2.00E+16
1.50E+16
1.00E+16
5.00E+15
0.00E+00
0
0.1
0.2
0.3
0.4
0.5
0.6
0.7
0.8
0.9
1
Time (s)

Figure 6

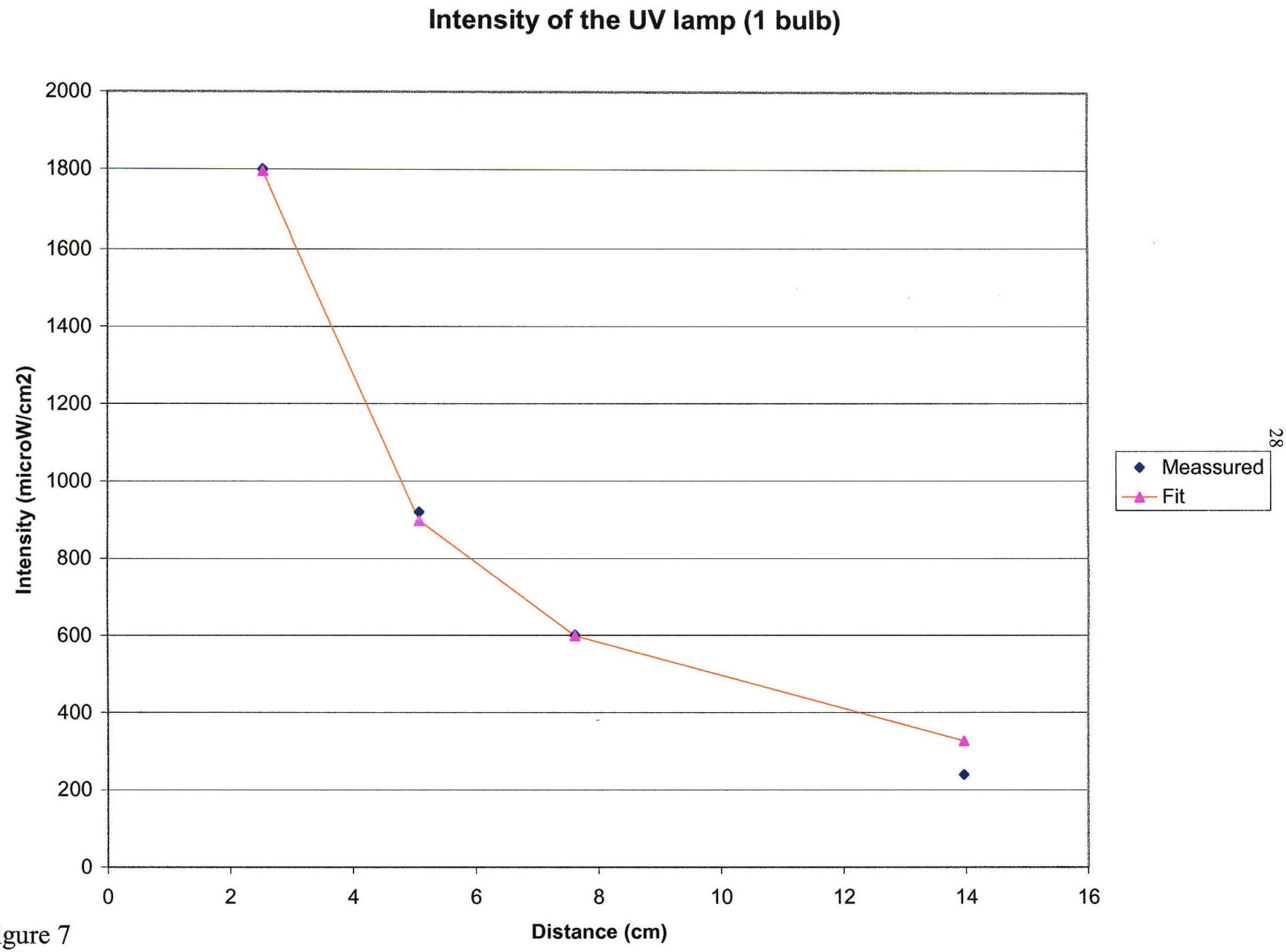
Intensity of the UV lamp (1 bulb)
Intensity (microW/cm2)
2000
1800
1600
1400
1200
1000
800
600
400
200
0
0
2
4
6
8
10
12
14
16
Distance (cm)
Meassured
Fit

Figure 7

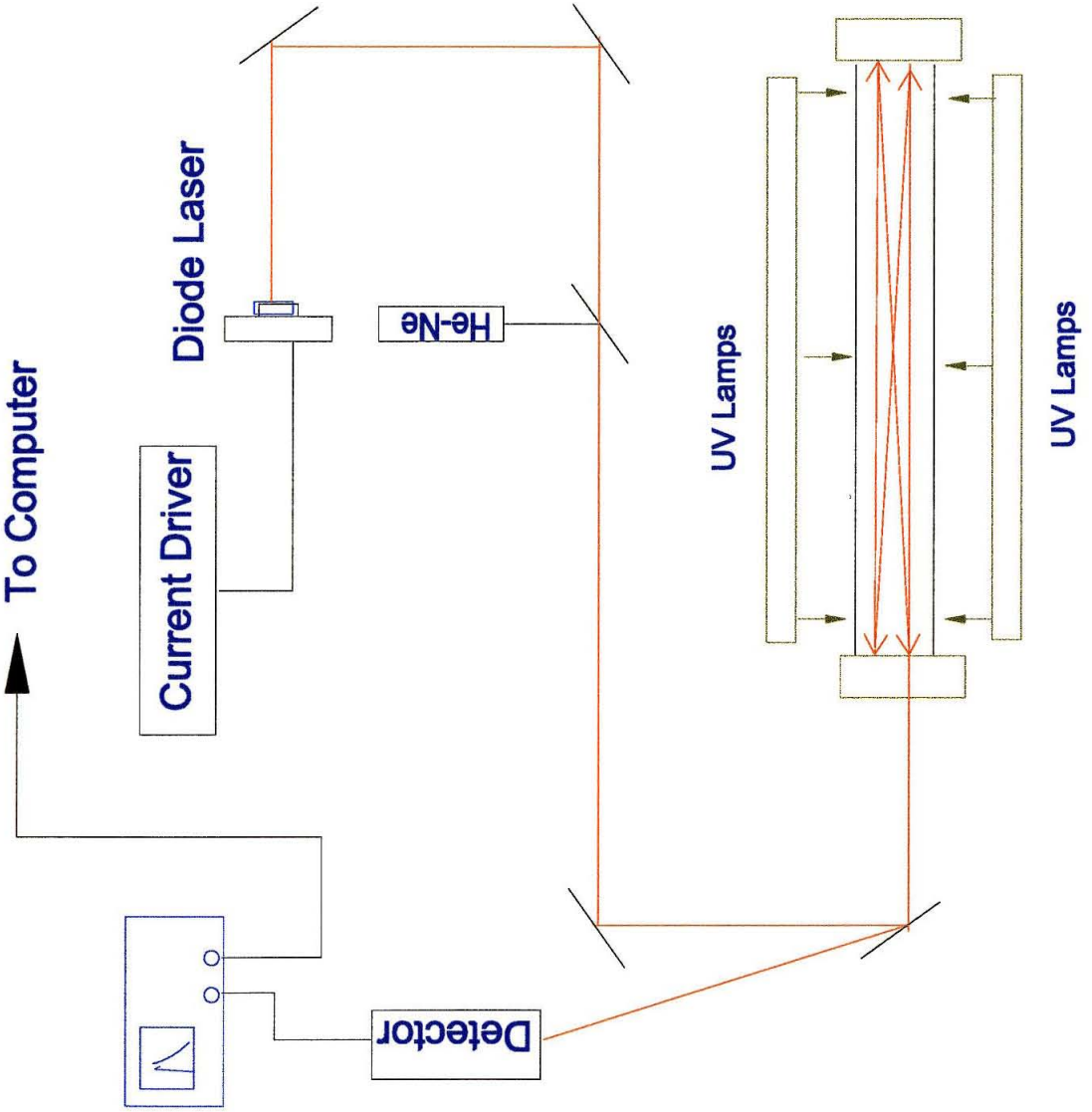
To Computer
Current Driver
Diode Laser
He-Ne
UV Lamps
UV Lamps
Detector

Figure 8

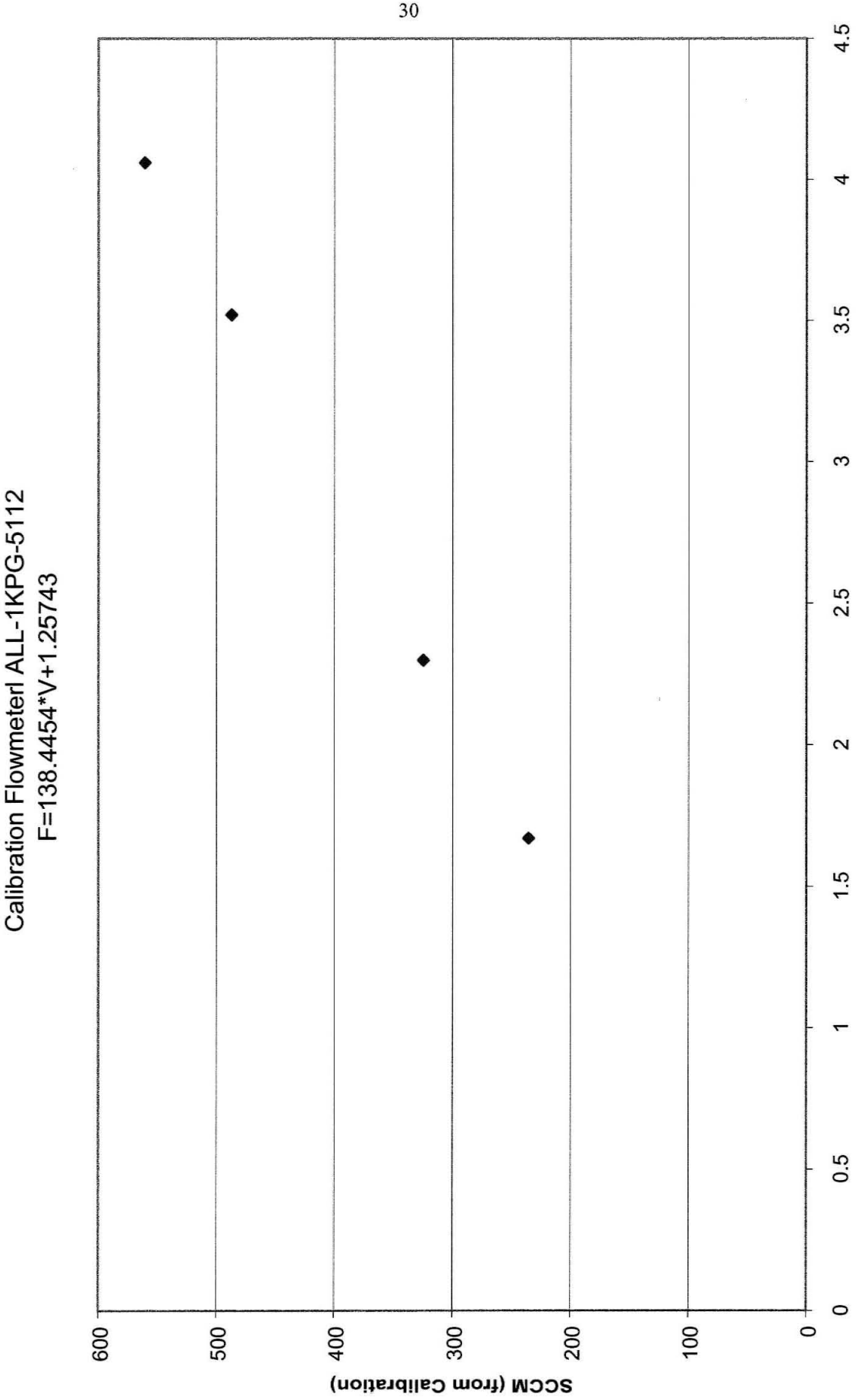
Calibration Flowmeterl ALL-1KPG-5112
F=138.4454*V+1.25743
SCCM (from Calibration)
600
500
400
300
200
100
0
0
0.5
1
1.5
2
2.5
3
3.5
4
4.5
Voltage (V)

Figure 9

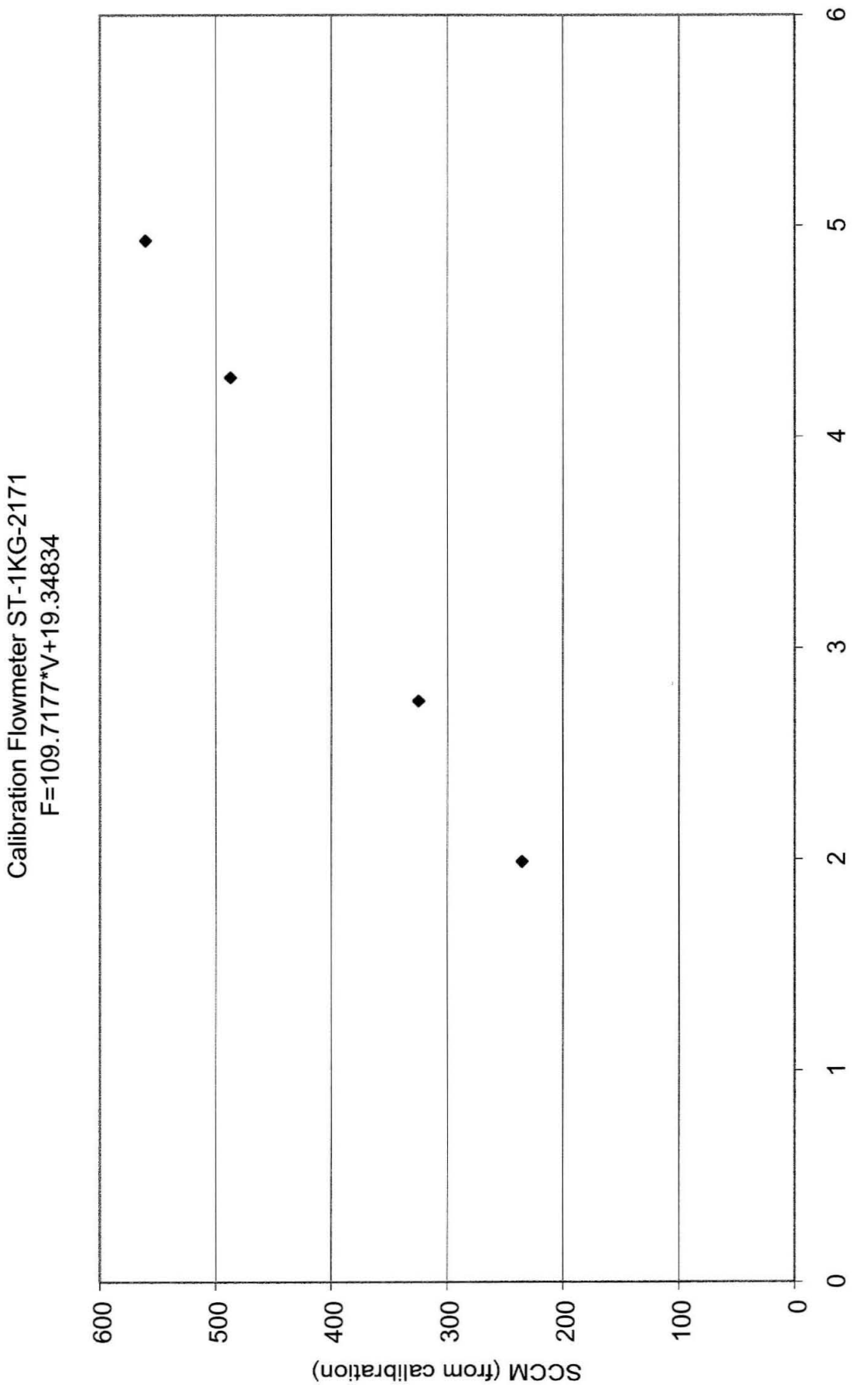
Calibration Flowmeter ST-1KG-2171
F=109.7177*V+19.34834
SCCM (from calibration)
600
500
400
300
200
100
0
0
1
2
3
4
5
6
Voltage (V)

Figure 10

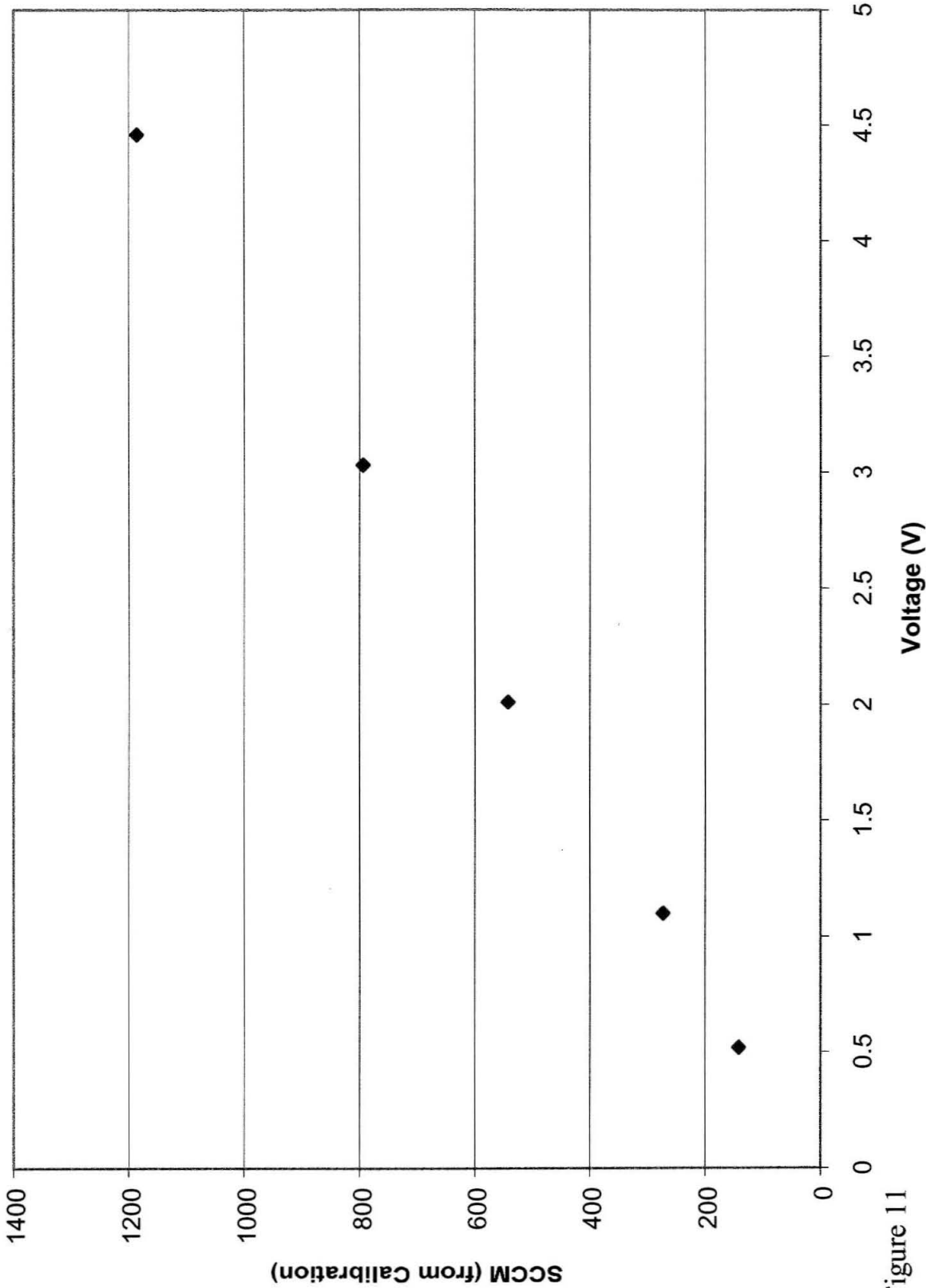
Calibration Flowmeter STM-136
F=266.37*V - 5.02
SCCM (from Calibration)
Voltage (V)
0
200
400
600
800
1000
1200
1400
0
0.5
1
1.5
2
2.5
3
3.5
4
4.5
5

Figure 11

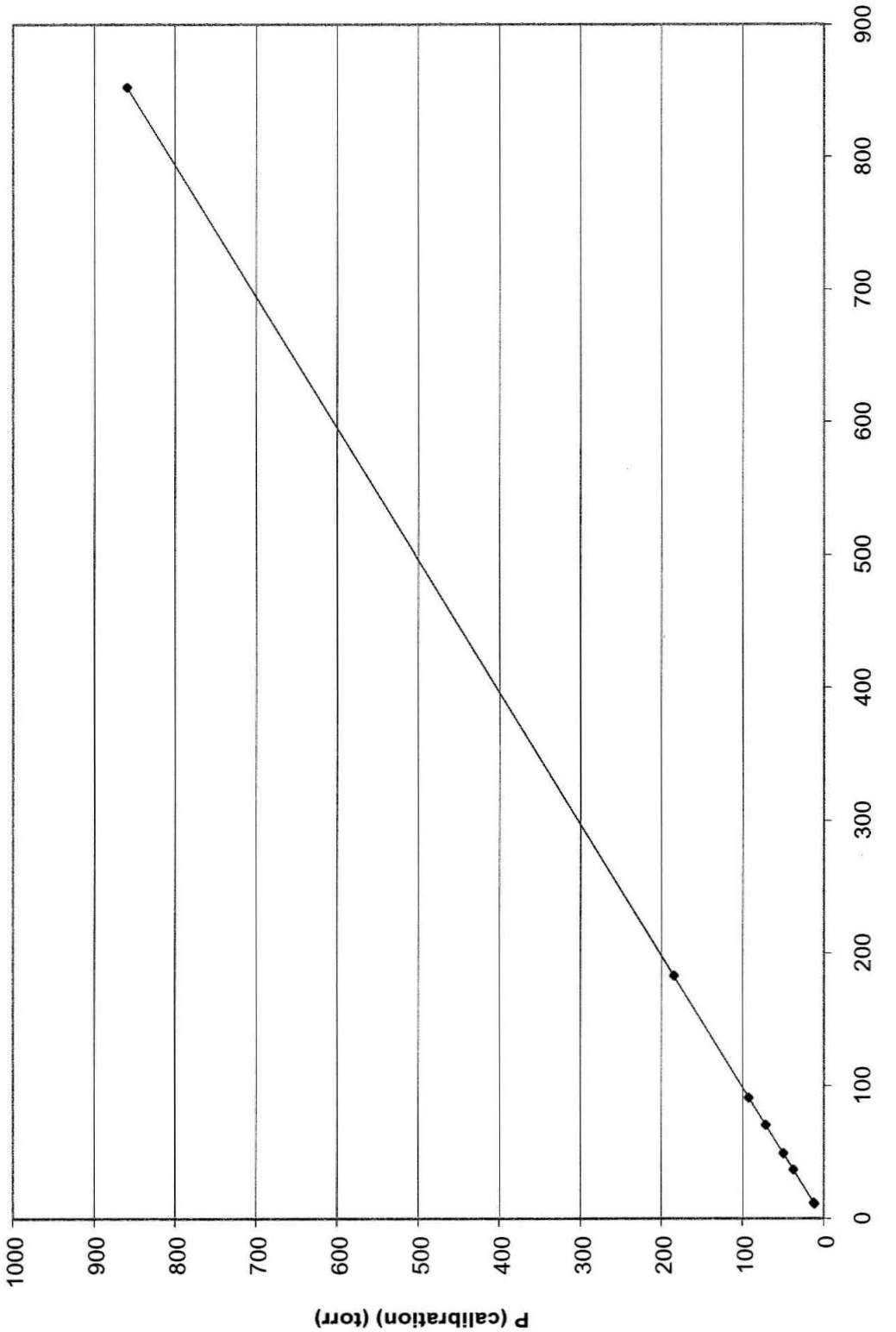
Calibration Curve for the Baratron (P.Number 002135)
P (calibration) (torr)
P Readout (torr)
0
100
200
300
400
500
600
700
800
900
1000

Figure 12

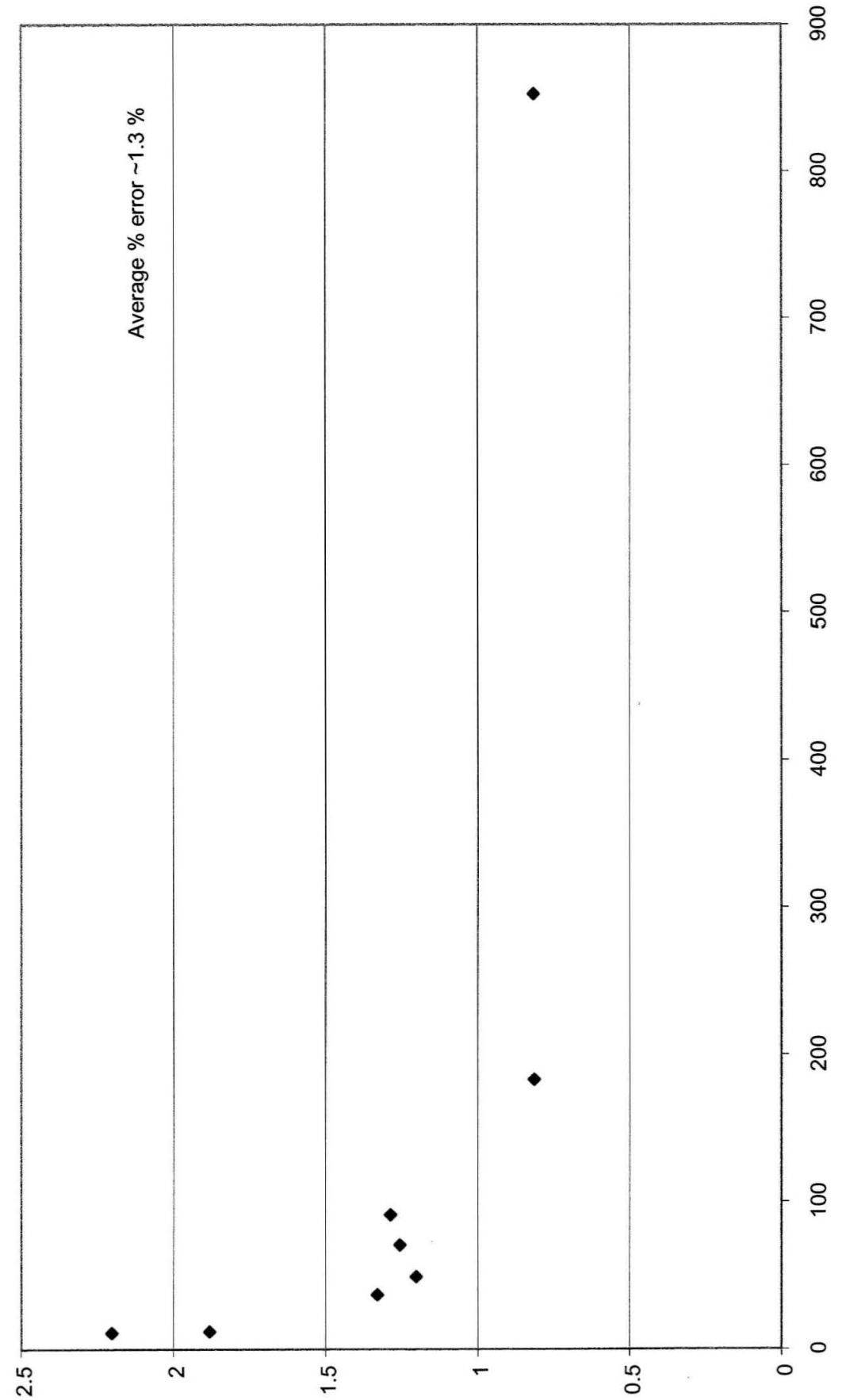
Error Percentage vs Pressure Readout
Average % error ~1.3 %
Error Percentage
P Readout (torr)
0
0.5
1
1.5
2
2.5
0
100
200
300
400
500
600
700
800
900

Figure 13

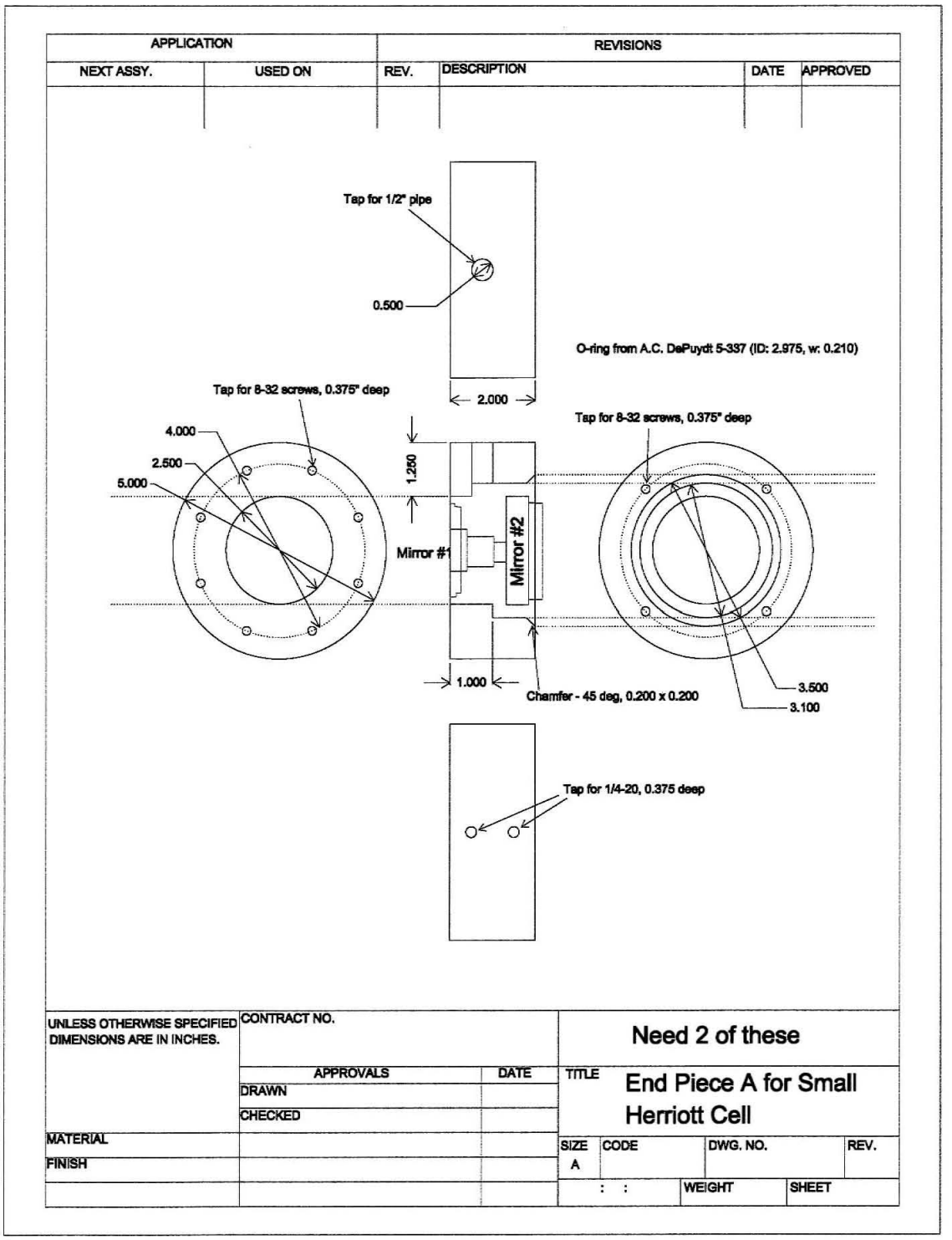
APPLICATION
NEXT ASSY.
USED ON
REVISIONS
REV.
DESCRIPTION
DATE
APPROVED
Tap for 1/2" pipe
0.500
O-ring from A.C. DePuydt 5-337 (ID: 2.975, w: 0.210)
2.000
Tap for 8-32 screws, 0.375" deep
4.000
2.500
5.000
1.250
Mirror #1
Mirror #2
Tap for 8-32 screws, 0.375" deep
1.000
Chamfer - 45 deg, 0.200 x 0.200
3.500
3.100
Tap for 1/4-20, 0.375 deep
UNLESS OTHERWISE SPECIFIED DIMENSIONS ARE IN INCHES.
CONTRACT NO.
APPROVALS
DATE
DRAWN
CHECKED
MATERIAL
FINISH
Need 2 of these
TITLE
End Piece A for Small Herriott Cell
SIZE
A
CODE
DWG. NO.
REV.
WEIGHT
SHEET

Figure 14

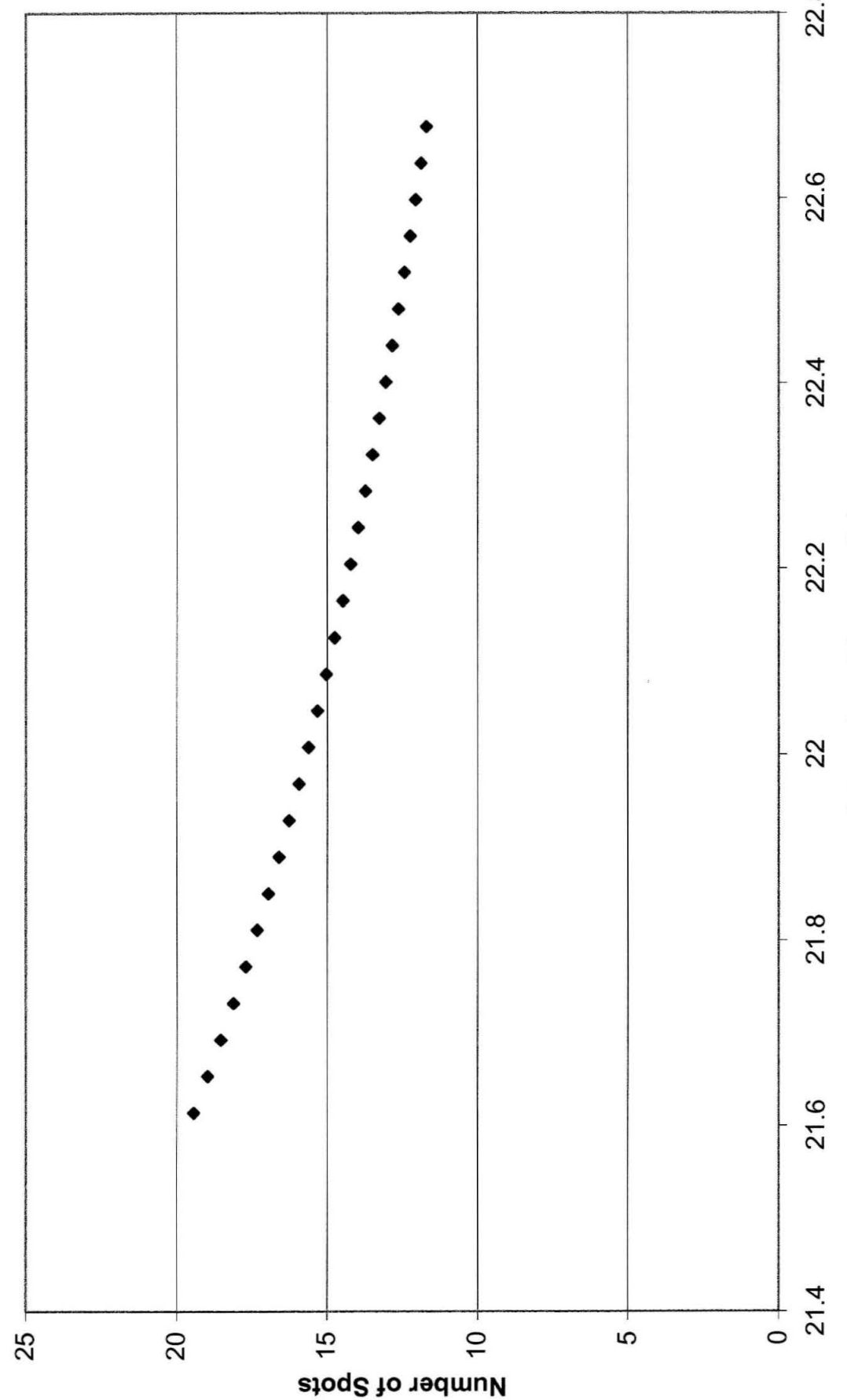
Number of Beam Spots vs Inter-mirror Distance
Number of Spots
25
20
15
10
5
0
21.4
21.6
21.8
22
22.2
22.4
22.6
22.8
Inter-mirror Distance (in)

Figure 15

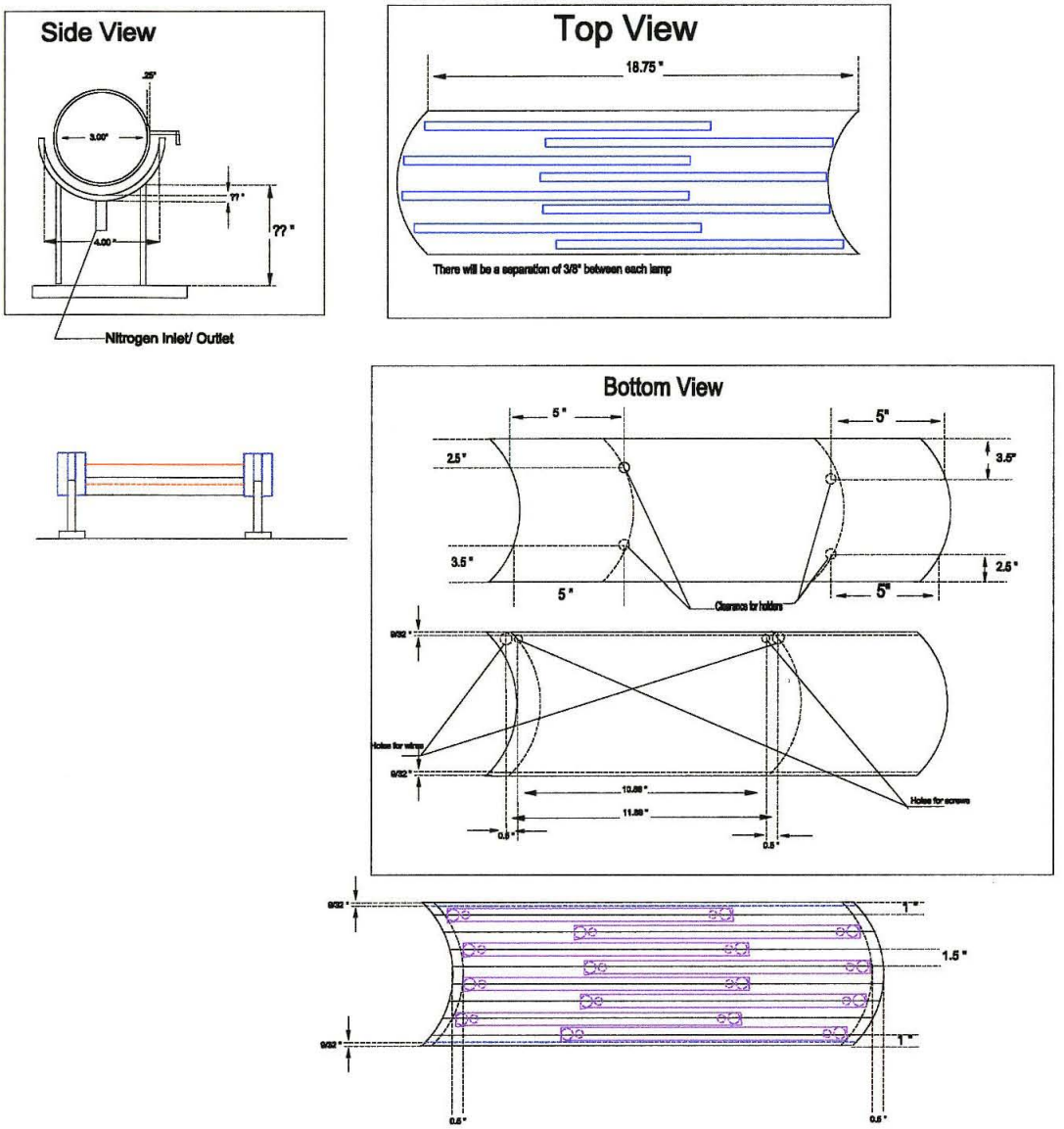
Side View
3.00"
??"
4.00"
Nitrogen Inlet/ Outlet
Top View
18.75"
There will be a separation of 3/8" between each lamp
Bottom View
5"
5"
2.5"
3.5"
3.5"
5"
5"
2.5"
Clearance for holders
Holes for wires
Holes for screws
1.5"
1"
1"

Figure 16

Appendix I. HO_2 Chemistry Simulation (FACSIMILE Program)

```
* HERRIOTT CELL CHEMISTRY;
*          by;
*            Fernando L. Rosario-Ortiz;
* Last modification:  May 29, 2001;
*     Ozone concentration ~ 1% of total oxygen concentration (ozoniser output at 20W);
* This simulation includes a photolysis rate for ozone of ~0.3 obtained;
* by measuring the UV flux for the lamps to be used and defining j as;
* the product of the Quantum Yield, cross section and flux (photons cm-2 s-1);
* for a single wavelength, which may give an underestimate of the real j value.;
* The system used is O3/O2/H2/N2, although the system composed of
CO/O3/O2/H2O/N2;
* gives similar results;
*
* O3 Cross section (@254 nm) =1150 e-20 cm2;
* HO2 Cross section (@ 250 nm) = 60e-20 cm2;
* H2O2 Cross section (@ 255 nm) = 67e-20 cm2;
*;
* Numerical values for the rate contants at 298 K are given below (the units were
omitted);
* K1  = 0.3;          O3 → O2 + O(1D)
* K2  = 2.6E-11;      O(1D) + N2 → O + N2
* K3  = 4.0E-11;      O(1D) + O2 → O + O2
* K4  = 1.0E-10;      O(1D) + H2 → OH + H
* K5  = 6.7E-15;      OH + H2 → H2O + H
* K6  = 2.2E-10;      O(1D) + H2O → OH + OH
* K7  = 3.3E-11;      O + OH → O2 + H
* K8  = 6.1e-14;      H + O2 → HO2
* K9  = 2.9E-11;      H + O3 → OH + O2
* K10 = 1.9E-12;      OH + OH → H2O + O
* K11 = 1.1E-10;      OH + HO2 → H2O + O
* K12 = 5.9e-13;      OH + OH → H2O2
* K13 = 1.7E-12;      HO2 + HO2 → H2O2 + O2
* K14 = 6.9e-16;      O + O2 → O3
* K15 = 5.9E-11;      O + HO2 → OH + O2
* K16 = 4.96E-12;     H2O2 + OH → H2O + HO2
* K17 = 2.5E-15;      HO2 + O3 → OH + 2 O2
* K18 = 0.2;          HO2 → Products (Wall Reaction)
* K19 = 6.8E-14;      OH + O3 → HO2 + O2
*;
* Lifetime of HO2, defined as 1/([HO2*K13]) is ~0.06 sec.;
* This approximation was made ignoring the wall reactions which will be fairly slow.;
*;
```

```
* Variables;
VARIABLE OD O3 O2 H2O OH O H;
VARIABLE  HO2 H2O2 N2 H2;
PARAMETER K1 K2 K3 K4 K5 K6 K7 K8;
PARAMETER K9 K10 K11 K12 K13 K14 K15 K16 K17 K18 P K19;
PARAMETER A12 B12 F12 HL12;
PARAMETER M T A8 B8 F8 HL8;

COMPILE INITIAL;
T = 298.0;
O3 = 3D16;
O2 = 8D17;
H2 = 3D17;
N2 = 1D17;
M = (O3+O2+N2+H2)*(273.15/T);
A12 = 6.2D-31*(300/T);
B12 = 2.6D-11;
F12 = (1 + (LOG10((A12*M)/B12))@2)@-1;
HL12 = A12*M/(1+A12*M/B12);
K12 = HL12*0.6@F12;
A8 = 5.7D-32*(T/300)@-1.6;
B8 = 7.5D-11;
F8 = (1 + (LOG10((A8*M)/B8))@2)@-1;
HL8 = A8*M/(1+A8*M/B8);
K8 = HL8*0.6@F8;
K14 = 6D-34*((T/300)@-2.3)*M;
**;
COMPILE EQUATIONS;
K1 % 0.3                        :O3 = OD + O2;
K2 % 1.8D-11*EXP(110/T)         :OD + N2 = O + N2;
K3 % 3.2D-11*EXP(70/T)          :OD + O2 = O + O2;
K4 % 1.0E-10                    :OD + H2 = OH + H;
K5 % 5.5D-12*EXP(-2000/T)       :OH + H2 = H2O + H;
K6 % 2.2D-10                    :OD + H2O = OH + OH;
K7 % 2.2D-11*EXP(120/T)         :O + OH = O2 + H;
%K8                             :H + O2 = HO2;
K9 % 1.4D-10*EXP(-470/T)        :H + O3 = OH + O2;
K10 % 4.2D-12*EXP(-240/T)       :OH + OH = H2O + O;
K11 % 4.8D-11*EXP(250/T)        :OH + HO2 = H2O + O2;
%K12                            :OH + OH = H2O2;
K13 % 2.3D-13*EXP(600/T)        :HO2 + HO2 = H2O2 + O2;
%K14                            :O + O2 = O3;
K15 % 3.0D-11*EXP(200/T)        :O + HO2 = OH + O2;
K16 % 2.9D-12*EXP(160/T)        :H2O2 + OH = H2O + HO2;
```

```
K17 % 1.1D-14*EXP(-500/T)        :HO2 + O3 = OH + O2 + O2;
K18 % 0.2                        :HO2 = P;
K19 % 1.6D-12*EXP(-940/T)        :OH + O3 = HO2 + O2;
**;
* HO2 Cross section is in the order of 6x10-19 so any contributions from photolysis;
* of HO2 is negligible. This is also the case for H2O2;
PSTREAM 1 0;
**;
PSTREAM 3 9;
   TIME HO2 O3  H  OH;
**;
WHEN TIME = 0.0 + 0.001*100 % CALL OUT;
**;
COMPILE OUT;
   PSTREAM 1;
   PSTREAM 3;
**;

EXEC OPEN 7 "O3O2H2.PRM" NEW;
EXEC OPEN 9 "O3O2H2.FIT" NEW;
BEGIN;
STOP;
Output;
```

TIME	HO2	O_3	H	OH
0.0000	0.0000	3.0000E+16	0.0000	0.0000
1.0000E-03	4.0083E+12	2.9979E+16	1.1920E+10	3.1972E+12
2.0000E-03	7.4283E+12	2.9954E+16	1.2613E+10	3.4467E+12
3.0000E-03	9.0618E+12	2.9929E+16	1.2566E+10	3.4260E+12
4.0000E-03	9.8501E+12	2.9904E+16	1.2437E+10	3.3774E+12
5.0000E-03	1.0249E+13	2.9879E+16	1.2342E+10	3.3407E+12
6.0000E-03	1.0457E+13	2.9854E+16	1.2286E+10	3.3180E+12
7.0000E-03	1.0566E+13	2.9830E+16	1.2255E+10	3.3045E+12
8.0000E-03	1.0624E+13	2.9805E+16	1.2238E+10	3.2963E+12
9.0000E-03	1.0653E+13	2.9780E+16	1.2230E+10	3.2911E+12
1.0000E-02	1.0667E+13	2.9755E+16	1.2225E+10	3.2874E+12
1.1000E-02	1.0673E+13	2.9731E+16	1.2223E+10	3.2845E+12
1.2000E-02	1.0675E+13	2.9706E+16	1.2222E+10	3.2822E+12
1.3000E-02	1.0674E+13	2.9681E+16	1.2222E+10	3.2801E+12
1.4000E-02	1.0673E+13	2.9657E+16	1.2223E+10	3.2781E+12
1.5000E-02	1.0670E+13	2.9632E+16	1.2223E+10	3.2762E+12
1.6000E-02	1.0668E+13	2.9608E+16	1.2224E+10	3.2744E+12
1.7000E-02	1.0665E+13	2.9583E+16	1.2224E+10	3.2726E+12
1.8000E-02	1.0661E+13	2.9559E+16	1.2225E+10	3.2709E+12
1.9000E-02	1.0658E+13	2.9534E+16	1.2226E+10	3.2691E+12
2.0000E-02	1.0655E+13	2.9510E+16	1.2227E+10	3.2674E+12
2.1000E-02	1.0652E+13	2.9485E+16	1.2228E+10	3.2656E+12
2.2000E-02	1.0649E+13	2.9461E+16	1.2228E+10	3.2639E+12
2.3000E-02	1.0645E+13	2.9436E+16	1.2229E+10	3.2622E+12
2.4000E-02	1.0642E+13	2.9412E+16	1.2230E+10	3.2605E+12
2.5000E-02	1.0639E+13	2.9388E+16	1.2231E+10	3.2588E+12

2.6000E-02	1.0635E+13	2.9363E+16	1.2232E+10	3.2572E+12
2.7000E-02	1.0632E+13	2.9339E+16	1.2233E+10	3.2555E+12
2.8000E-02	1.0629E+13	2.9315E+16	1.2234E+10	3.2539E+12
2.9000E-02	1.0625E+13	2.9290E+16	1.2235E+10	3.2522E+12
3.0000E-02	1.0621E+13	2.9266E+16	1.2236E+10	3.2506E+12
3.1000E-02	1.0618E+13	2.9242E+16	1.2238E+10	3.2491E+12
3.2000E-02	1.0614E+13	2.9218E+16	1.2239E+10	3.2475E+12
3.3000E-02	1.0611E+13	2.9194E+16	1.2240E+10	3.2459E+12
3.4000E-02	1.0607E+13	2.9169E+16	1.2241E+10	3.2443E+12
3.5000E-02	1.0603E+13	2.9145E+16	1.2242E+10	3.2427E+12
3.6000E-02	1.0600E+13	2.9121E+16	1.2244E+10	3.2412E+12
3.7000E-02	1.0596E+13	2.9097E+16	1.2245E+10	3.2397E+12
3.8000E-02	1.0592E+13	2.9073E+16	1.2246E+10	3.2382E+12
3.9000E-02	1.0588E+13	2.9049E+16	1.2248E+10	3.2367E+12
4.0000E-02	1.0584E+13	2.9025E+16	1.2249E+10	3.2352E+12
4.1000E-02	1.0580E+13	2.9001E+16	1.2250E+10	3.2337E+12
4.2000E-02	1.0577E+13	2.8977E+16	1.2252E+10	3.2322E+12
4.3000E-02	1.0573E+13	2.8953E+16	1.2253E+10	3.2307E+12
4.4000E-02	1.0569E+13	2.8929E+16	1.2255E+10	3.2293E+12
4.5000E-02	1.0565E+13	2.8905E+16	1.2256E+10	3.2278E+12
4.6000E-02	1.0561E+13	2.8881E+16	1.2258E+10	3.2264E+12
4.7000E-02	1.0557E+13	2.8857E+16	1.2259E+10	3.2249E+12
4.8000E-02	1.0553E+13	2.8834E+16	1.2261E+10	3.2235E+12
4.9000E-02	1.0549E+13	2.8810E+16	1.2262E+10	3.2221E+12
5.0000E-02	1.0545E+13	2.8786E+16	1.2264E+10	3.2207E+12
5.1000E-02	1.0541E+13	2.8762E+16	1.2265E+10	3.2193E+12
5.2000E-02	1.0536E+13	2.8739E+16	1.2267E+10	3.2179E+12
5.3000E-02	1.0532E+13	2.8715E+16	1.2269E+10	3.2165E+12
5.4000E-02	1.0528E+13	2.8691E+16	1.2270E+10	3.2152E+12
5.5000E-02	1.0524E+13	2.8667E+16	1.2272E+10	3.2138E+12
5.6000E-02	1.0520E+13	2.8644E+16	1.2274E+10	3.2124E+12
5.7000E-02	1.0515E+13	2.8620E+16	1.2275E+10	3.2111E+12
5.8000E-02	1.0511E+13	2.8596E+16	1.2277E+10	3.2098E+12
5.9000E-02	1.0507E+13	2.8573E+16	1.2279E+10	3.2084E+12
6.0000E-02	1.0503E+13	2.8549E+16	1.2281E+10	3.2071E+12
6.1000E-02	1.0498E+13	2.8526E+16	1.2282E+10	3.2058E+12
6.2000E-02	1.0494E+13	2.8502E+16	1.2284E+10	3.2045E+12
6.3000E-02	1.0490E+13	2.8479E+16	1.2286E+10	3.2032E+12
6.4000E-02	1.0485E+13	2.8455E+16	1.2288E+10	3.2019E+12
6.5000E-02	1.0481E+13	2.8432E+16	1.2290E+10	3.2006E+12
6.6000E-02	1.0477E+13	2.8408E+16	1.2291E+10	3.1993E+12
6.7000E-02	1.0472E+13	2.8385E+16	1.2293E+10	3.1980E+12
6.8000E-02	1.0468E+13	2.8361E+16	1.2295E+10	3.1968E+12
6.9000E-02	1.0463E+13	2.8338E+16	1.2297E+10	3.1955E+12
7.0000E-02	1.0459E+13	2.8315E+16	1.2299E+10	3.1942E+12
7.1000E-02	1.0454E+13	2.8291E+16	1.2301E+10	3.1930E+12
7.2000E-02	1.0450E+13	2.8268E+16	1.2303E+10	3.1917E+12
7.3000E-02	1.0446E+13	2.8245E+16	1.2305E+10	3.1905E+12
7.4000E-02	1.0441E+13	2.8221E+16	1.2307E+10	3.1893E+12
7.5000E-02	1.0436E+13	2.8198E+16	1.2309E+10	3.1880E+12
7.6000E-02	1.0432E+13	2.8175E+16	1.2311E+10	3.1868E+12
7.7000E-02	1.0427E+13	2.8152E+16	1.2313E+10	3.1856E+12
7.8000E-02	1.0423E+13	2.8129E+16	1.2315E+10	3.1844E+12
7.9000E-02	1.0418E+13	2.8105E+16	1.2317E+10	3.1832E+12
8.0000E-02	1.0414E+13	2.8082E+16	1.2319E+10	3.1820E+12
8.1000E-02	1.0409E+13	2.8059E+16	1.2321E+10	3.1808E+12
8.2000E-02	1.0404E+13	2.8036E+16	1.2323E+10	3.1796E+12
8.3000E-02	1.0400E+13	2.8013E+16	1.2325E+10	3.1785E+12
8.4000E-02	1.0395E+13	2.7990E+16	1.2327E+10	3.1773E+12

8.5000E-02	1.0390E+13	2.7967E+16	1.2330E+10	3.1761E+12
8.6000E-02	1.0386E+13	2.7944E+16	1.2332E+10	3.1749E+12
8.7000E-02	1.0381E+13	2.7921E+16	1.2334E+10	3.1738E+12
8.8000E-02	1.0376E+13	2.7898E+16	1.2336E+10	3.1726E+12
8.9000E-02	1.0372E+13	2.7875E+16	1.2338E+10	3.1715E+12
9.0000E-02	1.0367E+13	2.7852E+16	1.2340E+10	3.1703E+12
9.1000E-02	1.0362E+13	2.7829E+16	1.2343E+10	3.1692E+12
9.2000E-02	1.0358E+13	2.7806E+16	1.2345E+10	3.1680E+12
9.3000E-02	1.0353E+13	2.7783E+16	1.2347E+10	3.1669E+12
9.4000E-02	1.0348E+13	2.7760E+16	1.2349E+10	3.1658E+12
9.5000E-02	1.0343E+13	2.7737E+16	1.2351E+10	3.1646E+12
9.6000E-02	1.0339E+13	2.7714E+16	1.2354E+10	3.1635E+12
9.7000E-02	1.0334E+13	2.7692E+16	1.2356E+10	3.1624E+12
9.8000E-02	1.0329E+13	2.7669E+16	1.2358E+10	3.1613E+12
9.9000E-02	1.0324E+13	2.7646E+16	1.2361E+10	3.1602E+12
1.0000E-01	1.0319E+13	2.7623E+16	1.2363E+10	3.1591E+12

Appendix II. HO_2 Overtone Simulation

```
Asyrotwin Phase I

HO2-overtone

Lower State (A-Reduction)
  A          2.04502300D+01      A-K      1.94564125D+01
  B          1.02063500D+00      A-J      9.93817500D-01
  C          9.67000000D-01      a        2.68175000D-02
  D-K        4.10000000D-03
  D-JK       1.20000000D-04
  D-J        5.33000000D-06
  Kappa     -9.94494239D-01
  Defect     9.17858151D-02
Upper State (A-Reduction)
  A          1.82120000D+01      A-K      1.71252000D+01
  B          1.11700000D+00      A-J      1.08680000D+00
  C          1.05660000D+00      a        3.02000000D-02
  D-K        3.20000000D-03
  D-JK       1.20000000D-04
  D-J        5.20000000D-06
  Kappa     -9.92958485D-01
  Defect    -6.29134808D-02
 Band Origin:     6649.00000
 Representation: 1r    J range:    0 to    40    Maximum Ka: 40
 Nuclear Statistical Weights:  ee:  1   eo:  1   oo:  1 oe:  1
 Temperature:  298.0K
 Band Type: A+B   Delta-K order: 5   Decimal Output: 3
 Absorption Spectrum Calculation
 Intensity Ratio (B/A): 0.400    Intensity Minimum:  0.800
 No Negative Frequency Codes Defined

Number of observed lines accepted including those with
frequencies less than zero =      0

Calculated lines =    517
Observed lines with frequencies greater than zero =      0
Output in <filename>.eiv
Phase I Completed

Asyrotwin Phase II

HO2-overtone

                Upper          Lower                  Obs.       Calc.    Obs.-
 T P B DK   J  Ka  Kc    J  Ka  Kc    Int      Freq       Freq    Calc.
Comment
 A E R 0   27   1  26   26   1  25   0.82                6771.854
 A E R 0   27   0  27   26   0  26   0.95                6771.195
 A O R 0   27   1  27   26   1  26   0.90                6767.938
 A E R 0   26   1  25   25   1  24   1.01                6764.821
 A E R 0   26   0  26   25   0  25   1.17                6764.394
 A O R 0   26   1  26   25   1  25   1.10                6761.124
 A E R 0   25   1  24   24   1  23   1.24                6757.969
```

A	E	R	0	25	0	25	24	0	24	1.43	6757.763
A	O	R	0	25	1	25	24	1	24	1.34	6754.487
A	E	R	0	24	0	24	23	0	23	1.72	6751.301
A	E	R	0	24	1	23	23	1	22	1.50	6751.298
A	E	R	0	25	2	23	24	2	22	0.96	6750.416
A	O	R	0	25	2	24	24	2	23	0.97	6749.329
A	O	R	0	24	1	24	23	1	23	1.61	6748.027
A	E	R	0	23	0	23	22	0	22	2.05	6745.010
A	E	R	0	23	1	22	22	1	21	1.80	6744.808
A	E	R	0	24	2	22	23	2	21	1.16	6743.693
A	O	R	0	24	2	23	23	2	22	1.17	6742.750
A	O	R	0	23	1	23	22	1	22	1.92	6741.743
A	E	R	0	22	0	22	21	0	21	2.42	6738.889
A	E	R	0	22	1	21	21	1	20	2.13	6738.501
B	O	Q	1	11	3	9	11	2	10	0.81	6737.332
B	E	Q	1	11	3	8	11	2	9	0.81	6737.253
A	E	R	0	23	2	21	22	2	20	1.38	6737.164
A	O	R	0	23	2	22	22	2	21	1.40	6736.352
A	O	R	0	22	1	22	21	1	21	2.26	6735.637
B	O	Q	1	10	3	8	10	2	9	0.81	6735.290
B	E	Q	1	10	3	7	10	2	8	0.82	6735.236
B	E	R	1	19	1	19	18	0	18	0.86	6733.618
A	E	R	0	21	0	21	20	0	20	2.82	6732.940
A	E	R	0	21	1	20	20	1	19	2.49	6732.377
A	E	R	0	22	2	20	21	2	19	1.63	6730.829
A	O	R	0	22	2	21	21	2	20	1.64	6730.135
A	O	R	0	21	1	21	20	1	20	2.63	6729.709
B	E	R	1	18	1	18	17	0	17	0.96	6728.630
A	E	R	0	20	0	20	19	0	19	3.25	6727.163
A	E	R	0	20	1	19	19	1	18	2.87	6726.436
A	E	R	0	23	3	20	22	3	19	0.86	6724.991
A	O	R	0	23	3	21	22	3	20	0.86	6724.956
A	E	R	0	21	2	19	20	2	18	1.91	6724.688
A	O	R	0	21	2	20	20	2	19	1.92	6724.100
A	O	R	0	20	1	20	19	1	19	3.02	6723.958
B	E	R	1	17	1	17	16	0	16	1.06	6723.806
B	O	Q	1	15	2	14	15	1	15	0.86	6723.456
B	E	Q	1	17	2	15	17	1	16	0.87	6722.875
A	E	R	0	19	0	19	18	0	18	3.70	6721.559
A	E	R	0	19	1	18	18	1	17	3.28	6720.678
B	O	Q	1	14	2	13	14	1	14	0.94	6720.273
B	E	Q	1	16	2	14	16	1	15	0.95	6720.048
B	E	R	1	16	1	16	15	0	15	1.16	6719.145
A	E	R	0	20	2	18	19	2	17	2.20	6718.741
A	E	R	0	22	3	19	21	3	18	1.02	6718.734
A	O	R	0	22	3	20	21	3	19	1.02	6718.707
A	O	R	0	19	1	19	18	1	18	3.43	6718.386
A	O	R	0	20	2	19	19	2	18	2.21	6718.246
B	E	Q	1	15	2	13	15	1	14	1.02	6717.402
B	O	Q	1	13	2	12	13	1	13	1.00	6717.302
A	E	R	0	18	0	18	17	0	17	4.16	6716.128
A	E	R	0	18	1	17	17	1	16	3.70	6715.105
B	E	Q	1	14	2	12	14	1	13	1.08	6714.933
B	E	R	1	15	1	15	14	0	14	1.24	6714.646
B	O	Q	1	12	2	11	12	1	12	1.05	6714.544

A	O	R	0	18	1	18	17	1	17	3.85	6712.992
A	E	R	0	19	2	17	18	2	16	2.50	6712.987
A	E	R	0	21	3	18	20	3	17	1.19	6712.664
A	O	R	0	21	3	19	20	3	18	1.19	6712.643
B	E	Q	1	13	2	11	13	1	12	1.13	6712.640
A	O	R	0	19	2	18	18	2	17	2.51	6712.575
B	O	Q	1	11	2	10	11	1	11	1.08	6711.998
B	E	Q	1	20	1	19	20	0	20	0.94	6711.993
A	E	R	0	17	0	17	16	0	16	4.62	6710.873
B	E	Q	1	12	2	10	12	1	11	1.17	6710.521
B	E	R	1	14	1	14	13	0	13	1.32	6710.308
A	E	R	0	17	1	16	16	1	15	4.12	6709.717
B	O	Q	1	10	2	9	10	1	10	1.10	6709.664
B	E	Q	1	11	2	9	11	1	10	1.19	6708.572
A	O	R	0	17	1	17	16	1	16	4.27	6707.776
B	E	Q	1	19	1	18	19	0	19	1.10	6707.581
B	O	Q	1	9	2	8	9	1	9	1.09	6707.542
A	E	R	0	18	2	16	17	2	15	2.81	6707.425
A	O	R	0	18	2	17	17	2	16	2.82	6707.085
B	E	Q	1	10	2	8	10	1	9	1.19	6706.793
A	E	R	0	20	3	17	19	3	16	1.36	6706.780
A	O	R	0	20	3	18	19	3	17	1.36	6706.764
B	E	R	1	13	1	13	12	0	12	1.39	6706.131
A	E	R	0	16	0	16	15	0	15	5.07	6705.792
B	O	Q	1	8	2	7	8	1	8	1.06	6705.633
B	E	Q	1	9	2	7	9	1	8	1.16	6705.182
A	E	R	0	16	1	15	15	1	14	4.52	6704.513
B	O	Q	1	7	2	6	7	1	7	1.00	6703.936
B	E	Q	1	8	2	6	8	1	7	1.12	6703.736
B	E	Q	1	18	1	17	18	0	18	1.27	6703.398
A	O	R	0	16	1	16	15	1	15	4.67	6702.739
B	E	Q	1	7	2	5	7	1	6	1.04	6702.455
B	O	Q	1	6	2	5	6	1	6	0.92	6702.451
B	E	R	1	12	1	12	11	0	11	1.43	6702.112
A	E	R	0	17	2	15	16	2	14	3.12	6702.055
A	O	R	0	17	2	16	16	2	15	3.13	6701.778
B	E	Q	1	6	2	4	6	1	5	0.95	6701.336
B	O	Q	1	5	2	4	5	1	5	0.81	6701.179
A	E	R	0	19	3	16	18	3	15	1.55	6701.083
A	O	R	0	19	3	17	18	3	16	1.55	6701.071
A	E	R	0	15	0	15	14	0	14	5.48	6700.888
B	O	R	-1	18	0	18	17	1	17	0.85	6700.490
B	E	Q	1	5	2	3	5	1	4	0.83	6700.380
A	E	R	0	15	1	14	14	1	13	4.90	6699.495
B	E	Q	1	17	1	16	17	0	17	1.45	6699.442
B	E	R	1	11	1	11	10	0	10	1.46	6698.253
A	O	R	0	15	1	15	14	1	14	5.04	6697.882
A	E	R	0	16	2	14	15	2	13	3.42	6696.877
A	O	R	0	16	2	15	15	2	14	3.43	6696.654
A	E	R	0	14	0	14	13	0	13	5.85	6696.162
B	E	Q	1	16	1	15	16	0	16	1.63	6695.713
A	E	R	0	18	3	15	17	3	14	1.74	6695.571
A	O	R	0	18	3	16	17	3	15	1.74	6695.562
B	O	R	-1	17	0	17	16	1	16	0.92	6694.843
A	E	R	0	14	1	13	13	1	12	5.24	6694.662

B	E	R	1	10	1	10	9	0	9	1.46	6694.551
A	O	R	0	14	1	14	13	1	13	5.36	6693.203
B	E	Q	1	15	1	14	15	0	15	1.80	6692.209
A	E	R	0	15	2	13	14	2	12	3.70	6691.890
A	O	R	0	15	2	14	14	2	13	3.70	6691.713
A	E	R	0	13	0	13	12	0	12	6.15	6691.613
B	E	R	1	9	1	9	8	0	8	1.44	6691.006
A	E	R	0	17	3	14	16	3	13	1.93	6690.245
A	O	R	0	17	3	15	16	3	14	1.93	6690.239
A	E	R	0	13	1	12	12	1	11	5.51	6690.016
B	O	R	-1	16	0	16	15	1	15	1.00	6689.386
B	E	Q	1	14	1	13	14	0	14	1.97	6688.929
A	O	R	0	13	1	13	12	1	12	5.63	6688.704
B	E	R	1	8	1	8	7	0	7	1.40	6687.618
A	E	R	0	12	0	12	11	0	11	6.37	6687.243
A	E	R	0	14	2	12	13	2	11	3.94	6687.094
A	O	R	0	14	2	13	13	2	12	3.94	6686.955
B	E	Q	1	13	1	12	13	0	13	2.12	6685.873
A	E	R	0	12	1	11	11	1	10	5.71	6685.556
A	E	R	0	16	3	13	15	3	12	2.10	6685.105
A	O	R	0	16	3	14	15	3	13	2.10	6685.101
B	E	R	1	7	1	7	6	0	6	1.32	6684.387
A	O	R	0	12	1	12	11	1	11	5.81	6684.385
B	O	R	-1	15	0	15	14	1	14	1.06	6684.124
A	E	R	0	11	0	11	10	0	10	6.49	6683.052
B	E	Q	1	12	1	11	12	0	12	2.24	6683.039
A	E	R	0	13	2	11	12	2	10	4.13	6682.487
A	O	R	0	13	2	12	12	2	11	4.13	6682.380
B	E	R	1	6	1	6	5	0	5	1.22	6681.311
A	E	R	0	11	1	10	10	1	9	5.82	6681.282
B	E	Q	1	11	1	10	11	0	11	2.33	6680.427
A	O	R	0	11	1	11	10	1	10	5.90	6680.246
A	E	R	0	15	3	12	14	3	11	2.27	6680.151
A	O	R	0	15	3	13	14	3	12	2.27	6680.148
A	E	R	0	18	4	14	17	4	13	0.89	6679.355
A	O	R	0	18	4	15	17	4	14	0.89	6679.355
B	O	R	-1	14	0	14	13	1	13	1.11	6679.056
A	E	R	0	10	0	10	9	0	9	6.49	6679.042
B	E	R	1	5	1	5	4	0	4	1.09	6678.391
A	E	R	0	12	2	10	11	2	9	4.26	6678.069
B	E	Q	1	10	1	9	10	0	10	2.39	6678.035
A	O	R	0	12	2	11	11	2	10	4.26	6677.989
A	E	R	0	10	1	9	9	1	8	5.82	6677.196
A	O	R	0	10	1	10	9	1	9	5.89	6676.288
B	E	Q	1	9	1	8	9	0	9	2.39	6675.864
B	E	R	1	4	1	4	3	0	3	0.95	6675.627
A	E	R	0	14	3	11	13	3	10	2.40	6675.382
A	O	R	0	14	3	12	13	3	11	2.40	6675.380
A	E	R	0	9	0	9	8	0	8	6.37	6675.213
B	O	R	-1	13	0	13	12	1	12	1.14	6674.186
A	E	R	0	17	4	13	16	4	12	0.98	6674.036
A	O	R	0	17	4	14	16	4	13	0.98	6674.036
B	E	Q	1	8	1	7	8	0	8	2.35	6673.912
A	E	R	0	11	2	9	10	2	8	4.31	6673.841
A	O	R	0	11	2	10	10	2	9	4.31	6673.782

A	E	R	0	9	1	8	8	1	7	5.70	6673.297
A	O	R	0	9	1	9	8	1	8	5.76	6672.510
B	E	Q	1	7	1	6	7	0	7	2.25	6672.178
A	E	R	0	8	0	8	7	0	7	6.12	6671.566
A	E	R	0	13	3	10	12	3	9	2.51	6670.799
A	O	R	0	13	3	11	12	3	10	2.51	6670.797
B	E	Q	1	6	1	5	6	0	6	2.10	6670.662
A	E	R	0	10	2	8	9	2	7	4.28	6669.801
A	O	R	0	10	2	9	9	2	8	4.28	6669.758
A	E	R	0	8	1	7	7	1	6	5.46	6669.585
B	O	R	-1	12	0	12	11	1	11	1.16	6669.516
B	E	Q	1	5	1	4	5	0	5	1.89	6669.364
A	O	R	0	8	1	8	7	1	7	5.50	6668.913
A	E	R	0	16	4	12	15	4	11	1.06	6668.902
A	O	R	0	16	4	13	15	4	12	1.06	6668.902
B	E	Q	1	4	1	3	4	0	4	1.63	6668.283
A	E	R	0	7	0	7	6	0	6	5.72	6668.101
B	E	Q	1	3	1	2	3	0	3	1.32	6667.418
B	E	Q	1	2	1	1	2	0	2	0.97	6666.770
A	E	R	0	12	3	9	11	3	8	2.57	6666.401
A	O	R	0	12	3	10	11	3	9	2.57	6666.400
A	E	R	0	7	1	6	6	1	5	5.09	6666.061
A	E	R	0	9	2	7	8	2	6	4.16	6665.949
A	O	R	0	9	2	8	8	2	7	4.16	6665.919
A	O	R	0	7	1	7	6	1	6	5.12	6665.496
B	O	R	-1	11	0	11	10	1	10	1.16	6665.046
A	E	R	0	6	0	6	5	0	5	5.20	6664.819
A	E	R	0	15	4	11	14	4	10	1.14	6663.952
A	O	R	0	15	4	12	14	4	11	1.14	6663.952
A	E	R	0	6	1	5	5	1	4	4.59	6662.725
A	E	R	0	8	2	6	7	2	5	3.94	6662.284
A	O	R	0	8	2	7	7	2	6	3.94	6662.265
A	O	R	0	6	1	6	5	1	5	4.61	6662.261
A	E	R	0	11	3	8	10	3	7	2.59	6662.188
A	O	R	0	11	3	9	10	3	8	2.59	6662.188
A	E	R	0	5	0	5	4	0	4	4.54	6661.721
B	O	R	-1	10	0	10	9	1	9	1.13	6660.779
A	E	R	0	5	1	4	4	1	3	3.96	6659.578
A	O	R	0	5	1	5	4	1	4	3.98	6659.208
A	E	R	0	14	4	10	13	4	9	1.20	6659.188
A	O	R	0	14	4	11	13	4	10	1.20	6659.188
B	E	Q	-1	19	0	19	19	1	18	0.94	6659.072
A	E	R	0	7	2	5	6	2	4	3.61	6658.807
A	E	R	0	4	0	4	3	0	3	3.78	6658.807
A	O	R	0	7	2	6	6	2	5	3.61	6658.795
A	E	R	0	10	3	7	9	3	6	2.54	6658.161
A	O	R	0	10	3	8	9	3	7	2.54	6658.161
A	E	P	0	25	0	25	26	0	26	0.92	6657.692
B	O	R	-1	9	0	9	8	1	8	1.09	6656.717
A	E	R	0	4	1	3	3	1	2	3.22	6656.618
B	E	P	1	5	1	5	6	0	6	0.83	6656.540
A	O	R	0	4	1	4	3	1	3	3.23	6656.336
B	E	Q	-1	18	0	18	18	1	17	1.09	6656.186
A	E	R	0	3	0	3	2	0	2	2.91	6656.077
A	E	R	0	6	2	4	5	2	3	3.17	6655.517

A	O	R	0	6	2	5	5	2	4	3.17	6655.510
B	E	P	1	6	1	6	7	0	7	0.94	6655.494
A	O	P	0	25	1	25	26	1	26	0.87	6655.346
A	E	P	0	24	0	24	25	0	25	1.13	6655.062
A	E	R	0	13	4	9	12	4	8	1.25	6654.609
A	O	R	0	13	4	10	12	4	9	1.25	6654.609
B	E	P	1	7	1	7	8	0	8	1.02	6654.606
A	E	R	0	9	3	6	8	3	5	2.44	6654.320
A	O	R	0	9	3	7	8	3	6	2.44	6654.319
B	E	P	1	16	1	16	17	0	17	0.83	6653.910
B	E	P	1	8	1	8	9	0	9	1.08	6653.877
A	E	R	0	3	1	2	2	1	1	2.36	6653.848
A	O	R	0	3	1	3	2	1	2	2.36	6653.646
A	E	R	0	2	0	2	1	0	1	1.98	6653.533
B	E	Q	-1	17	0	17	17	1	16	1.25	6653.439
A	E	P	0	24	1	23	25	1	24	0.98	6653.376
B	E	P	1	15	1	15	16	0	16	0.90	6653.326
B	E	P	1	9	1	9	10	0	10	1.11	6653.309
B	E	P	1	14	1	14	15	0	15	0.97	6652.910
B	E	P	1	10	1	10	11	0	11	1.12	6652.903
B	O	R	-1	8	0	8	7	1	7	1.02	6652.860
A	O	P	0	24	1	24	25	1	25	1.06	6652.712
B	E	P	1	13	1	13	14	0	14	1.03	6652.661
B	E	P	1	11	1	11	12	0	12	1.11	6652.658
A	E	P	0	23	0	23	24	0	24	1.37	6652.612
B	E	P	1	12	1	12	13	0	13	1.08	6652.577
A	E	R	0	5	2	3	4	2	2	2.62	6652.413
A	O	R	0	5	2	4	4	2	3	2.62	6652.409
A	E	R	0	2	1	1	1	1	0	1.35	6651.266
A	E	R	0	1	0	1	0	0	0	1.00	6651.174
A	O	R	0	2	1	2	1	1	1	1.35	6651.138
B	E	Q	-1	16	0	16	16	1	15	1.41	6650.832
A	E	P	0	23	1	22	24	1	23	1.19	6650.823
A	E	R	0	8	3	5	7	3	4	2.26	6650.663
A	O	R	0	8	3	6	7	3	5	2.26	6650.663
A	E	P	0	22	0	22	23	0	23	1.65	6650.344
A	O	P	0	23	1	23	24	1	24	1.29	6650.262
A	E	R	0	12	4	8	11	4	7	1.27	6650.214
A	O	R	0	12	4	9	11	4	8	1.27	6650.214
A	E	R	0	4	2	2	3	2	1	1.95	6649.496
A	O	R	0	4	2	3	3	2	2	1.95	6649.494
B	O	R	-1	7	0	7	6	1	6	0.92	6649.211
A	E	P	0	22	1	21	23	1	22	1.44	6648.460
B	E	Q	-1	15	0	15	15	1	14	1.57	6648.368
A	E	P	0	21	0	21	22	0	22	1.96	6648.257
A	O	P	0	22	1	22	23	1	23	1.55	6647.996
A	E	R	0	7	3	4	6	3	3	2.01	6647.192
A	O	R	0	7	3	5	6	3	4	2.01	6647.192
A	E	P	0	0	0	0	1	0	1	0.99	6647.012
A	O	Q	0	1	1	0	1	1	1	1.35	6646.913
A	E	Q	0	1	1	1	1	1	0	1.35	6646.799
A	E	R	0	3	2	1	2	2	0	1.11	6646.765
A	O	R	0	3	2	2	2	2	1	1.11	6646.765
A	E	P	0	20	0	20	21	0	21	2.31	6646.352
A	E	P	0	21	1	20	22	1	21	1.72	6646.288

B	E	Q-1	14	0	14	14	1	13	1.73	6646.049
A	E	R 0	11	4	7	10	4	6	1.26	6646.005
A	O	R 0	11	4	8	10	4	7	1.26	6646.005
A	O	P 0	21	1	21	22	1	22	1.84	6645.915
B	O	R-1	6	0	6	5	1	5	0.81	6645.770
A	E	P 0	1	0	1	2	0	2	1.94	6645.211
A	E	P 0	19	0	19	20	0	20	2.69	6644.629
A	E	P 0	20	1	19	21	1	20	2.03	6644.305
A	O	P 0	20	1	20	21	1	21	2.16	6644.018
A	E	P 0	23	2	21	24	2	22	0.92	6643.956
A	E	R 0	6	3	3	5	3	2	1.68	6643.907
A	O	R 0	6	3	4	5	3	3	1.68	6643.907
B	E	Q-1	13	0	13	13	1	12	1.87	6643.876
A	O	P 0	23	2	22	24	2	23	0.93	6643.612
A	E	P 0	2	0	2	3	0	3	2.83	6643.596
A	E	P 0	18	0	18	19	0	19	3.09	6643.088
A	O	P 0	1	1	1	2	1	2	1.33	6642.931
A	E	P 0	1	1	0	2	1	1	1.33	6642.831
A	E	P 0	19	1	18	20	1	19	2.37	6642.513
A	O	Q 0	5	2	3	5	2	4	0.87	6642.485
A	E	Q 0	5	2	4	5	2	3	0.87	6642.475
A	O	P 0	19	1	19	20	1	20	2.50	6642.305
A	E	P 0	3	0	3	4	0	4	3.63	6642.167
A	E	R 0	10	4	6	9	4	5	1.22	6641.981
A	O	R 0	10	4	7	9	4	6	1.22	6641.981
B	E	Q-1	12	0	12	12	1	11	1.99	6641.850
A	E	P 0	17	0	17	18	0	18	3.51	6641.731
A	E	P 0	22	2	20	23	2	21	1.11	6641.573
A	O	Q 0	4	2	2	4	2	3	1.12	6641.552
A	E	Q 0	4	2	3	4	2	2	1.12	6641.548
A	O	P 0	2	1	2	3	1	3	2.29	6641.336
A	O	P 0	22	2	21	23	2	22	1.12	6641.291
A	E	P 0	2	1	1	3	1	2	2.29	6641.196
A	E	P 0	4	0	4	5	0	5	4.33	6640.926
A	E	P 0	18	1	17	19	1	18	2.73	6640.911
A	E	R 0	5	3	2	4	3	1	1.25	6640.807
A	O	R 0	5	3	3	4	3	2	1.25	6640.807
A	O	Q 0	3	2	1	3	2	2	1.51	6640.806
A	E	Q 0	3	2	2	3	2	1	1.51	6640.805
A	O	P 0	18	1	18	19	1	19	2.87	6640.777
A	E	P 0	16	0	16	17	0	17	3.93	6640.558
A	O	Q 0	2	2	0	2	2	1	2.23	6640.248
A	E	Q 0	2	2	1	2	2	0	2.23	6640.247
B	E	Q-1	11	0	11	11	1	10	2.08	6639.974
A	O	P 0	3	1	3	4	1	4	3.11	6639.924
A	E	P 0	5	0	5	6	0	6	4.91	6639.871
A	E	P 0	3	1	2	4	1	3	3.10	6639.750
A	E	P 0	15	0	15	16	0	16	4.35	6639.568
A	E	P 0	17	1	16	18	1	17	3.11	6639.499
A	O	P 0	17	1	17	18	1	18	3.25	6639.432
A	E	P 0	21	2	19	22	2	20	1.33	6639.385
A	O	P 0	21	2	20	22	2	21	1.33	6639.158
A	E	P 0	6	0	6	7	0	7	5.35	6639.002
A	E	P 0	14	0	14	15	0	15	4.75	6638.763
A	O	P 0	4	1	4	5	1	5	3.79	6638.696

A	E	P	0	4	1	3	5	1	4	3.78	6638.495
A	E	P	0	7	0	7	8	0	8	5.66	6638.320
A	E	P	0	16	1	15	17	1	16	3.49	6638.279
A	O	P	0	16	1	16	17	1	17	3.63	6638.272
B	E	Q	-1	10	0	10	10	1	9	2.13	6638.250
A	E	P	0	13	0	13	14	0	14	5.12	6638.143
A	E	R	0	9	4	5	8	4	4	1.14	6638.142
A	O	R	0	9	4	6	8	4	5	1.14	6638.142
A	E	P	0	8	0	8	9	0	9	5.85	6637.825
A	E	P	0	12	0	12	13	0	13	5.44	6637.708
A	O	P	0	5	1	5	6	1	6	4.35	6637.650
A	E	P	0	9	0	9	10	0	10	5.90	6637.517
A	E	P	0	11	0	11	12	0	12	5.68	6637.458
A	E	P	0	5	1	4	6	1	5	4.33	6637.430
A	E	P	0	10	0	10	11	0	11	5.84	6637.394
A	E	P	0	20	2	18	21	2	19	1.56	6637.394
A	O	P	0	15	1	15	16	1	16	4.01	6637.296
A	E	P	0	15	1	14	16	1	15	3.87	6637.249
A	O	P	0	20	2	19	21	2	20	1.57	6637.213
A	O	P	0	6	1	6	7	1	7	4.79	6636.788
B	E	Q	-1	9	0	9	9	1	8	2.15	6636.677
A	E	P	0	6	1	5	7	1	6	4.75	6636.555
A	O	P	0	14	1	14	15	1	15	4.37	6636.504
A	E	P	0	14	1	13	15	1	14	4.24	6636.409
A	O	P	0	7	1	7	8	1	8	5.10	6636.110
A	O	P	0	13	1	13	14	1	14	4.70	6635.896
A	E	P	0	7	1	6	8	1	7	5.05	6635.870
A	E	P	0	13	1	12	14	1	13	4.57	6635.760
A	O	P	0	8	1	8	9	1	9	5.29	6635.615
A	E	P	0	19	2	17	20	2	18	1.82	6635.597
A	O	P	0	12	1	12	13	1	13	4.98	6635.472
A	O	P	0	19	2	18	20	2	19	1.82	6635.456
A	E	P	0	8	1	7	9	1	8	5.23	6635.375
A	O	P	0	9	1	9	10	1	10	5.36	6635.303
A	E	P	0	12	1	11	13	1	12	4.86	6635.302
B	E	Q	-1	8	0	8	8	1	7	2.11	6635.258
A	O	P	0	11	1	11	12	1	12	5.19	6635.232
A	O	P	0	10	1	10	11	1	11	5.32	6635.176
A	E	P	0	9	1	8	10	1	9	5.28	6635.071
A	E	P	0	11	1	10	12	1	11	5.08	6635.035
A	E	P	0	10	1	9	11	1	10	5.23	6634.958
A	E	R	0	8	4	4	7	4	3	1.03	6634.488
A	O	R	0	8	4	5	7	4	4	1.03	6634.488
A	O	P	0	2	2	1	3	2	2	1.08	6634.288
A	E	P	0	2	2	0	3	2	1	1.08	6634.288
A	E	P	0	18	2	16	19	2	17	2.09	6633.995
B	E	Q	-1	7	0	7	7	1	6	2.03	6633.994
A	O	P	0	18	2	17	19	2	18	2.10	6633.887
B	E	Q	-1	6	0	6	6	1	5	1.90	6632.886
A	O	P	0	3	2	2	4	2	3	1.87	6632.860
A	E	P	0	3	2	1	4	2	2	1.87	6632.859
A	E	P	0	17	2	15	18	2	16	2.37	6632.587
A	O	P	0	17	2	16	18	2	17	2.38	6632.506
A	O	Q	0	6	3	3	6	3	4	0.98	6631.998
A	E	Q	0	6	3	4	6	3	3	0.98	6631.998

B	E	Q-1	5	0	5	5	1	4	1.71	6631.934
A	O	P 0	4	2	3	5	2	4	2.50	6631.619
A	E	P 0	4	2	2	5	2	3	2.50	6631.617
A	E	P 0	16	2	14	17	2	15	2.66	6631.371
A	O	P 0	16	2	15	17	2	16	2.66	6631.313
B	E	Q-1	4	0	4	4	1	3	1.47	6631.140
A	E	R 0	7	4	3	6	4	2	0.86	6631.019
A	O	R 0	7	4	4	6	4	3	0.86	6631.019
A	O	Q 0	5	3	2	5	3	3	1.23	6630.882
A	E	Q 0	5	3	3	5	3	2	1.23	6630.882
A	O	P 0	5	2	4	6	2	5	3.00	6630.564
A	E	P 0	5	2	3	6	2	4	3.00	6630.562
B	E	Q-1	3	0	3	3	1	2	1.20	6630.503
A	E	P 0	15	2	13	16	2	14	2.94	6630.348
A	O	P 0	15	2	14	16	2	15	2.94	6630.307
B	E	Q-1	2	0	2	2	1	1	0.88	6630.026
A	O	Q 0	4	3	1	4	3	2	1.58	6629.952
A	E	Q 0	4	3	2	4	3	1	1.58	6629.952
A	O	P 0	6	2	5	7	2	6	3.38	6629.696
A	E	P 0	6	2	4	7	2	5	3.38	6629.693
A	E	P 0	14	2	12	15	2	13	3.20	6629.516
A	O	P 0	14	2	13	15	2	14	3.21	6629.490
A	O	Q 0	3	3	0	3	3	1	2.13	6629.208
A	E	Q 0	3	3	1	3	3	0	2.13	6629.208
A	O	P 0	7	2	6	8	2	7	3.65	6629.015
A	E	P 0	7	2	5	8	2	6	3.65	6629.012
A	E	P 0	13	2	11	14	2	12	3.44	6628.876
A	O	P 0	13	2	12	14	2	13	3.45	6628.860
A	O	P 0	8	2	7	9	2	8	3.82	6628.521
A	E	P 0	8	2	6	9	2	7	3.82	6628.518
A	E	P 0	12	2	10	13	2	11	3.64	6628.426
A	O	P 0	12	2	11	13	2	12	3.65	6628.417
A	O	P 0	9	2	8	10	2	9	3.89	6628.214
A	E	P 0	9	2	7	10	2	8	3.89	6628.212
A	E	P 0	11	2	9	12	2	10	3.79	6628.165
A	O	P 0	11	2	10	12	2	11	3.80	6628.162
A	O	P 0	10	2	9	11	2	10	3.88	6628.094
A	E	P 0	10	2	8	11	2	9	3.88	6628.094
A	E	P 0	21	3	18	22	3	19	0.83	6627.661
A	O	P 0	21	3	19	22	3	20	0.83	6627.650
A	E	P 0	20	3	17	21	3	18	0.97	6625.699
A	O	P 0	20	3	18	21	3	19	0.97	6625.691
B	O	P-1	16	0	16	17	1	17	0.85	6624.919
A	E	P 0	19	3	16	20	3	17	1.13	6623.927
A	O	P 0	19	3	17	20	3	18	1.13	6623.922
B	O	P-1	15	0	15	16	1	16	0.93	6623.538
B	O	P-1	3	0	3	4	1	4	0.83	6622.984
B	O	P-1	14	0	14	15	1	15	1.01	6622.357
A	E	P 0	18	3	15	19	3	16	1.29	6622.346
A	O	P 0	18	3	16	19	3	17	1.29	6622.343
B	O	P-1	4	0	4	5	1	5	0.95	6621.876
B	O	P-1	13	0	13	14	1	14	1.08	6621.378
B	O	P-1	5	0	5	6	1	6	1.05	6620.980
A	E	P 0	17	3	14	18	3	15	1.46	6620.955
A	O	P 0	17	3	15	18	3	16	1.46	6620.953

B	O	P-1	12	0	12	13	1	13	1.14	6620.602
B	O	P-1	6	0	6	7	1	7	1.13	6620.297
B	O	P-1	11	0	11	12	1	12	1.19	6620.031
A	O	P 0	4	3	2	5	3	3	1.19	6620.027
A	E	P 0	4	3	1	5	3	2	1.19	6620.027
B	O	P-1	7	0	7	8	1	8	1.19	6619.824
A	E	P 0	16	3	13	17	3	14	1.64	6619.754
A	O	P 0	16	3	14	17	3	15	1.64	6619.752
B	O	P-1	10	0	10	11	1	11	1.22	6619.667
B	O	P-1	8	0	8	9	1	9	1.22	6619.562
B	O	P-1	9	0	9	10	1	10	1.23	6619.510
A	O	P 0	5	3	3	6	3	4	1.58	6618.973
A	E	P 0	5	3	2	6	3	3	1.58	6618.973
A	E	P 0	15	3	12	16	3	13	1.81	6618.741
A	O	P 0	15	3	13	16	3	14	1.81	6618.740
A	O	P 0	6	3	4	7	3	5	1.88	6618.106
A	E	P 0	6	3	3	7	3	4	1.88	6618.106
A	E	P 0	14	3	11	15	3	12	1.96	6617.918
A	O	P 0	14	3	12	15	3	13	1.96	6617.918
A	O	P 0	7	3	5	8	3	6	2.09	6617.426
A	E	P 0	7	3	4	8	3	5	2.09	6617.426
A	E	P 0	13	3	10	14	3	11	2.10	6617.284
A	O	P 0	13	3	11	14	3	12	2.10	6617.283
A	O	P 0	8	3	6	9	3	7	2.24	6616.933
A	E	P 0	8	3	5	9	3	6	2.24	6616.933
A	E	P 0	12	3	9	13	3	10	2.21	6616.838
A	O	P 0	12	3	10	13	3	11	2.21	6616.837
A	O	P 0	9	3	7	10	3	8	2.31	6616.628
A	E	P 0	9	3	6	10	3	7	2.31	6616.628
A	E	P 0	11	3	8	12	3	9	2.29	6616.580
A	O	P 0	11	3	9	12	3	10	2.29	6616.580
A	E	P 0	10	3	7	11	3	8	2.33	6616.510
A	O	P 0	10	3	8	11	3	9	2.33	6616.510
A	O	Q 0	6	4	2	6	4	3	0.91	6615.837
A	E	Q 0	6	4	3	6	4	2	0.91	6615.837
A	O	Q 0	5	4	1	5	4	2	1.14	6614.721
A	E	Q 0	5	4	2	5	4	1	1.14	6614.721
A	O	Q 0	4	4	0	4	4	1	1.46	6613.791
A	E	Q 0	4	4	1	4	4	0	1.46	6613.791
B	E	Q-1	13	1	12	13	2	11	0.83	6607.921
B	E	Q-1	12	1	11	12	2	10	0.86	6605.149
A	E	P 0	16	4	12	17	4	13	0.83	6603.617
A	O	P 0	16	4	13	17	4	14	0.83	6603.617
A	E	P 0	15	4	11	16	4	12	0.91	6602.604
A	O	P 0	15	4	12	16	4	13	0.91	6602.604
B	E	Q-1	11	1	10	11	2	9	0.88	6602.583
A	O	P 0	6	4	3	7	4	4	0.81	6601.957
A	E	P 0	6	4	2	7	4	3	0.81	6601.957
A	E	P 0	14	4	10	15	4	11	0.99	6601.780
A	O	P 0	14	4	11	15	4	12	0.99	6601.780
A	O	P 0	7	4	4	8	4	5	0.95	6601.279
A	E	P 0	7	4	3	8	4	4	0.95	6601.279
A	E	P 0	13	4	9	14	4	10	1.05	6601.145
A	O	P 0	13	4	10	14	4	11	1.05	6601.145
A	O	P 0	8	4	5	9	4	6	1.05	6600.788

```
 A E P 0   8   4   4    9   4   5   1.05              6600.788
 A E P 0  12   4   8   13   4   9   1.10              6600.698
 A O P 0  12   4   9   13   4  10   1.10              6600.698
 A E P 0   9   4   5   10   4   6   1.11              6600.484
 A O P 0   9   4   6   10   4   7   1.11              6600.484
 A E P 0  11   4   7   12   4   8   1.13              6600.439
 A O P 0  11   4   8   12   4   9   1.13              6600.439
 A E P 0  10   4   6   11   4   7   1.13              6600.367
 A O P 0  10   4   7   11   4   8   1.13              6600.367
 B E Q-1  10   1   9   10   2   8   0.88              6600.226
 B O Q-1  11   1  11   11   2  10   0.80              6598.677
 B E Q-1   9   1   8    9   2   7   0.86              6598.079
 B O Q-1  10   1  10   10   2   9   0.82              6596.960
 B E Q-1   8   1   7    8   2   6   0.83              6596.142
 B O Q-1   9   1   9    9   2   8   0.81              6595.398
Std. Dev. =  0.00000 for       0 lines with |Obs-Calc| less than
0.10000
Calculated lines =     517 Observed lines =       0
Temporary intensity minimum:  0.800
Output in <filename>.SUB
Output in <filename>.TMP
Phase II Completed

Asyrotwin Phase VII

HO2-overtone

Scale: Linear
Line shape: Lorentzian
Spectrum divided into  10000 intervals from  99999.000 to      0.000
Half width:  0.050
The linear intensity output has been scaled from 0.0 to 1.0
Output in <filename>.PLT
Phase VII Completed
```

Appendix III. HO_2 Electronic Simulation

```
Asyrotwin Phase I

HO2-electronic

Lower State (A-Reduction)
  A          2.04700000D+01      A-K      1.94800000D+01
  B          1.02000000D+00      A-J      9.90000000D-01
  C          9.60000000D-01      a        3.00000000D-02
  D-K        4.80000000D-03
  D-JK       1.39000000D-04
  D-J        4.10000000D-06
  d-K        9.42000000D-05
  d-J        2.33000000D-07
  Kappa     -9.93849308D-01
  Defect     2.09414454D-01
Upper State (A-Reduction)
  A          2.03400000D+01      A-K      1.92575000D+01
  B          1.11000000D+00      A-J      1.08250000D+00
  C          1.05500000D+00      a        2.75000000D-02
  D-K        4.11000000D-03
  D-JK       1.15000000D-04
  D-J        3.90000000D-06
  d-K        6.59000000D-05
  d-J        2.05000000D-07
  Kappa     -9.94296085D-01
  Defect    -3.70498840D-02
 Band Origin:    7030.00000
 Representation: 1r    J range:   0 to   60    Maximum Ka: 50
 Nuclear Statistical Weights:  ee:  1   eo:  1   oo:  1 oe:  1
 Temperature:  298.0K
 Band Type: C     Delta-K order: 1   Decimal Output: 3
 Absorption Spectrum Calculation
 Intensity Factor:   1.0    Intensity Minimum:  0.800
 No Negative Frequency Codes Defined

Number of observed lines accepted including those with
frequencies less than zero =      0

Calculated lines =    487
Observed lines with frequencies greater than zero =      0
Phase I Completed

Asyrotwin Phase II

HO2-electronic

                Upper          Lower                    Obs.        Calc.    Obs.-
 T P B DK   J   Ka   Kc    J   Ka   Kc     Int        Freq        Freq     Calc.
Comment
 C O R 1    9    5    5    8    4    5    0.80                  7224.453
 C E R 1    9    5    4    8    4    4    0.80                  7224.453
 C O R 1    8    5    4    7    4    4    0.83                  7220.828
 C E R 1    8    5    3    7    4    3    0.83                  7220.828
```

C	O	R	1	16	4	13	15	3	13	0.82	7218.708
C	E	R	1	16	4	12	15	3	12	0.82	7218.704
C	O	R	1	7	5	3	6	4	3	0.86	7217.385
C	E	R	1	7	5	2	6	4	2	0.86	7217.385
C	O	R	1	6	5	2	5	4	2	0.89	7214.125
C	E	R	1	6	5	1	5	4	1	0.89	7214.125
C	O	R	1	15	4	12	14	3	12	0.91	7213.802
C	E	R	1	15	4	11	14	3	11	0.91	7213.799
C	O	R	1	5	5	1	4	4	1	0.91	7211.049
C	E	R	1	5	5	0	4	4	0	0.91	7211.049
C	O	R	1	14	4	11	13	3	11	0.99	7209.078
C	E	R	1	14	4	10	13	3	10	0.99	7209.076
C	O	R	1	13	4	10	12	3	10	1.07	7204.536
C	E	R	1	13	4	9	12	3	9	1.07	7204.535
C	O	R	1	12	4	9	11	3	9	1.15	7200.177
C	E	R	1	12	4	8	11	3	8	1.15	7200.176
C	O	R	1	19	3	17	18	2	17	0.83	7197.808
C	E	R	1	19	3	16	18	2	16	0.83	7197.174
C	O	R	1	11	4	8	10	3	8	1.22	7196.000
C	E	R	1	11	4	7	10	3	7	1.22	7196.000
C	O	R	1	18	3	16	17	2	16	0.95	7192.308
C	O	R	1	10	4	7	9	3	7	1.28	7192.006
C	E	R	1	10	4	6	9	3	6	1.28	7192.006
C	E	R	1	18	3	15	17	2	15	0.95	7191.799
C	O	Q	1	17	4	13	17	3	15	0.83	7190.245
C	E	Q	1	17	4	14	17	3	14	0.83	7190.237
C	O	R	1	9	4	6	8	3	6	1.32	7188.195
C	E	R	1	9	4	5	8	3	5	1.32	7188.195
C	O	Q	1	16	4	12	16	3	14	0.92	7187.123
C	E	Q	1	16	4	13	16	3	13	0.92	7187.118
C	O	R	1	17	3	15	16	2	15	1.07	7186.997
C	E	R	1	17	3	14	16	2	14	1.07	7186.594
C	O	R	1	8	4	5	7	3	5	1.36	7184.566
C	E	R	1	8	4	4	7	3	4	1.36	7184.566
C	O	Q	1	15	4	11	15	3	13	1.00	7184.184
C	E	Q	1	15	4	12	15	3	12	1.00	7184.181
C	O	R	1	16	3	14	15	2	14	1.19	7181.874
C	E	R	1	16	3	13	15	2	13	1.19	7181.559
C	O	Q	1	14	4	10	14	3	12	1.07	7181.429
C	E	Q	1	14	4	11	14	3	11	1.07	7181.427
C	O	R	1	7	4	4	6	3	4	1.38	7181.121
C	E	R	1	7	4	3	6	3	3	1.38	7181.121
C	O	Q	1	13	4	9	13	3	11	1.13	7178.858
C	E	Q	1	13	4	10	13	3	10	1.13	7178.856
C	O	R	1	6	4	3	5	3	3	1.40	7177.859
C	E	R	1	6	4	2	5	3	2	1.40	7177.859
C	O	R	1	15	3	13	14	2	13	1.30	7176.938
C	E	R	1	15	3	12	14	2	12	1.30	7176.696
C	O	Q	1	12	4	8	12	3	10	1.17	7176.470
C	E	Q	1	12	4	9	12	3	9	1.17	7176.469
C	O	R	1	5	4	2	4	3	2	1.41	7174.780
C	E	R	1	5	4	1	4	3	1	1.41	7174.780
C	O	Q	1	11	4	7	11	3	9	1.19	7174.265
C	E	Q	1	11	4	8	11	3	8	1.19	7174.265
C	O	Q	1	10	4	6	10	3	8	1.18	7172.244

C	E	Q	1	10	4	7	10	3	7	1.18	7172.244
C	O	R	1	14	3	12	13	2	12	1.42	7172.188
C	E	R	1	14	3	11	13	2	11	1.42	7172.007
C	O	R	1	4	4	1	3	3	1	1.42	7171.884
C	E	R	1	4	4	0	3	3	0	1.42	7171.884
C	O	R	1	20	2	19	19	1	19	0.83	7171.392
C	O	Q	1	9	4	5	9	3	7	1.15	7170.407
C	E	Q	1	9	4	6	9	3	6	1.15	7170.407
C	O	Q	1	8	4	4	8	3	6	1.08	7168.753
C	E	Q	1	8	4	5	8	3	5	1.08	7168.753
C	O	R	1	13	3	11	12	2	11	1.52	7167.626
C	E	R	1	13	3	10	12	2	10	1.52	7167.492
C	O	Q	1	7	4	3	7	3	5	0.97	7167.283
C	E	Q	1	7	4	4	7	3	4	0.97	7167.283
C	E	R	1	21	2	19	20	1	19	0.88	7166.413
C	O	Q	1	6	4	2	6	3	4	0.81	7165.996
C	E	Q	1	6	4	3	6	3	3	0.81	7165.996
C	O	R	1	19	2	18	18	1	18	0.96	7165.166
C	O	Q	1	20	3	17	20	2	19	0.91	7164.091
C	O	R	1	12	3	10	11	2	10	1.62	7163.249
C	E	R	1	12	3	9	11	2	9	1.62	7163.154
C	E	Q	1	20	3	18	20	2	18	0.91	7163.108
C	E	R	1	20	2	18	19	1	18	1.01	7160.974
C	O	Q	1	19	3	16	19	2	18	1.05	7160.355
C	E	Q	1	19	3	17	19	2	17	1.05	7159.549
C	O	R	1	18	2	17	17	1	17	1.09	7159.154
C	O	R	1	11	3	9	10	2	9	1.69	7159.058
C	E	R	1	11	3	8	10	2	8	1.69	7158.992
C	O	Q	1	18	3	15	18	2	17	1.19	7156.811
C	E	Q	1	18	3	16	18	2	16	1.19	7156.158
C	E	R	1	19	2	17	18	1	17	1.14	7155.715
C	O	R	1	10	3	8	9	2	8	1.76	7155.053
C	E	R	1	10	3	7	9	2	7	1.76	7155.008
C	E	R	1	23	1	22	22	0	22	0.89	7154.176
C	O	Q	1	17	3	14	17	2	16	1.34	7153.458
C	O	R	1	17	2	16	16	1	16	1.23	7153.356
C	E	Q	1	17	3	15	17	2	15	1.34	7152.935
C	O	R	1	9	3	7	8	2	7	1.80	7151.232
C	E	R	1	9	3	6	8	2	6	1.80	7151.204
C	E	R	1	18	2	16	17	1	16	1.27	7150.635
C	O	Q	1	16	3	13	16	2	15	1.49	7150.296
C	E	Q	1	16	3	14	16	2	14	1.49	7149.883
C	O	R	1	16	2	15	15	1	15	1.36	7147.771
C	O	R	1	8	3	6	7	2	6	1.82	7147.596
C	E	R	1	8	3	5	7	2	5	1.82	7147.579
C	O	Q	1	15	3	12	15	2	14	1.63	7147.323
C	E	R	1	22	1	21	21	0	21	1.08	7147.172
C	E	Q	1	15	3	13	15	2	13	1.63	7147.002
C	E	R	1	17	2	15	16	1	15	1.41	7145.729
C	O	Q	1	14	3	11	14	2	13	1.75	7144.540
C	E	Q	1	14	3	12	14	2	12	1.75	7144.294
C	O	R	1	7	3	5	6	2	5	1.81	7144.145
C	E	R	1	7	3	4	6	2	4	1.81	7144.136
C	O	R	1	15	2	14	14	1	14	1.49	7142.401
C	O	Q	1	13	3	10	13	2	12	1.86	7141.944

C	E	Q	1	13	3	11	13	2	11	1.86	7141.760
C	E	R	1	16	2	14	15	1	14	1.54	7140.997
C	O	R	1	6	3	4	5	2	4	1.79	7140.878
C	E	R	1	6	3	3	5	2	3	1.79	7140.873
C	E	R	1	21	1	20	20	0	20	1.28	7140.400
C	O	Q	1	12	3	9	12	2	11	1.94	7139.537
C	E	Q	1	12	3	10	12	2	10	1.94	7139.402
C	O	Q	1	21	2	19	21	1	21	0.85	7138.075
C	O	R	1	5	3	3	4	2	3	1.75	7137.795
C	E	R	1	5	3	2	4	2	2	1.75	7137.793
C	O	Q	1	11	3	8	11	2	10	1.99	7137.317
C	O	R	1	14	2	13	13	1	13	1.62	7137.244
C	E	Q	1	11	3	9	11	2	9	1.99	7137.220
C	E	R	1	15	2	13	14	1	13	1.67	7136.436
C	O	Q	1	10	3	7	10	2	9	2.00	7135.283
C	E	Q	1	10	3	8	10	2	8	2.00	7135.216
C	O	R	1	4	3	2	3	2	2	1.70	7134.897
C	E	R	1	4	3	1	3	2	1	1.70	7134.896
C	E	R	1	20	1	19	19	0	19	1.50	7133.857
C	O	Q	1	9	3	6	9	2	8	1.97	7133.436
C	E	Q	1	9	3	7	9	2	7	1.97	7133.392
C	O	Q	1	20	2	18	20	1	20	1.01	7133.387
C	O	R	1	13	2	12	12	1	12	1.73	7132.301
C	O	R	1	3	3	1	2	2	1	1.67	7132.182
C	E	R	1	3	3	0	2	2	0	1.67	7132.182
C	E	R	1	14	2	12	13	1	12	1.78	7132.044
C	O	Q	1	8	3	5	8	2	7	1.89	7131.775
C	E	Q	1	8	3	6	8	2	6	1.89	7131.747
C	E	Q	1	23	2	22	23	1	22	0.82	7130.483
C	O	Q	1	7	3	4	7	2	6	1.75	7130.299
C	E	Q	1	7	3	5	7	2	5	1.75	7130.282
C	O	Q	1	6	3	3	6	2	5	1.56	7129.009
C	E	Q	1	6	3	4	6	2	4	1.56	7128.999
C	O	Q	1	19	2	17	19	1	19	1.19	7128.939
C	O	Q	1	5	3	2	5	2	4	1.31	7127.903
C	E	Q	1	5	3	3	5	2	3	1.31	7127.899
C	E	R	1	13	2	11	12	1	11	1.88	7127.819
C	O	R	1	12	2	11	11	1	11	1.82	7127.572
C	E	R	1	19	1	18	18	0	18	1.73	7127.542
C	O	Q	1	4	3	1	4	2	3	0.98	7126.982
C	E	Q	1	4	3	2	4	2	2	0.98	7126.980
C	E	Q	1	22	2	21	22	1	21	0.97	7126.873
C	O	Q	1	18	2	16	18	1	18	1.38	7124.727
C	E	R	1	12	2	10	11	1	10	1.96	7123.760
C	E	Q	1	21	2	20	21	1	20	1.14	7123.425
C	O	R	1	11	2	10	10	1	10	1.90	7123.056
C	E	R	1	18	1	17	17	0	17	1.98	7121.453
C	O	Q	1	17	2	15	17	1	17	1.58	7120.751
C	E	Q	1	20	2	19	20	1	19	1.32	7120.138
C	E	R	1	11	2	9	10	1	9	2.01	7119.865
C	O	R	1	10	2	9	9	1	9	1.95	7118.754
C	E	Q	1	19	2	18	19	1	18	1.51	7117.011
C	O	Q	1	16	2	14	16	1	16	1.78	7117.007
C	E	R	1	10	2	8	9	1	8	2.04	7116.132
C	E	R	1	17	1	16	16	0	16	2.24	7115.590

C O R 1	9	2	8	8	1	8	1.97	7114.666
C E Q 1	18	2	17	18	1	17	1.70	7114.044
C O Q 1	15	2	13	15	1	15	1.98	7113.494
C E R 1	9	2	7	8	1	7	2.05	7112.560
C E Q 1	27	1	27	27	0	27	0.96	7111.422
C E Q 1	17	2	16	17	1	16	1.90	7111.237
C O R 1	8	2	7	7	1	7	1.96	7110.791
C O Q 1	14	2	12	14	1	14	2.17	7110.211
C E R 1	16	1	15	15	0	15	2.49	7109.950
C E R 1	8	2	6	7	1	6	2.02	7109.147
C E Q 1	16	2	15	16	1	15	2.10	7108.588
C O Q 1	13	2	11	13	1	13	2.34	7107.154
C O R 1	7	2	6	6	1	6	1.91	7107.130
C E Q 1	26	1	26	26	0	26	1.18	7106.817
C E Q 1	15	2	14	15	1	14	2.29	7106.097
C E R 1	7	2	5	6	1	5	1.96	7105.893
C E R 1	15	1	14	14	0	14	2.73	7104.532
C O Q 1	12	2	10	12	1	12	2.47	7104.323
C E Q 1	14	2	13	14	1	13	2.46	7103.764
C O R 1	6	2	5	5	1	5	1.84	7103.683
C E R 1	6	2	4	5	1	4	1.87	7102.797
C E Q 1	25	1	25	25	0	25	1.43	7102.403
C O Q 1	11	2	9	11	1	11	2.58	7101.717
C E Q 1	13	2	12	13	1	12	2.60	7101.588
C O R 1	5	2	4	4	1	4	1.74	7100.449
C E R 1	5	2	3	4	1	3	1.76	7099.857
C E Q 1	12	2	11	12	1	11	2.71	7099.570
C E R 1	14	1	13	13	0	13	2.96	7099.336
C O Q 1	10	2	8	10	1	10	2.63	7099.333
C E Q 1	24	1	24	24	0	24	1.72	7098.180
C E Q 1	11	2	10	11	1	10	2.78	7097.708
C O R 1	4	2	3	3	1	3	1.61	7097.429
C O Q 1	9	2	7	9	1	9	2.64	7097.170
C E R 1	4	2	2	3	1	2	1.62	7097.073
C E Q 1	10	2	9	10	1	9	2.81	7096.002
C O Q 1	8	2	6	8	1	8	2.58	7095.226
C O R 1	3	2	2	2	1	2	1.47	7094.623
C E Q 1	9	2	8	9	1	8	2.78	7094.452
C E R 1	3	2	1	2	1	1	1.48	7094.445
C E R 1	13	1	12	12	0	12	3.16	7094.359
C E Q 1	23	1	23	23	0	23	2.04	7094.146
C O Q 1	7	2	5	7	1	7	2.45	7093.502
C E R-1	22	0	22	21	1	20	0.83	7093.090
C E Q 1	8	2	7	8	1	7	2.69	7093.058
C O R 1	2	2	1	1	1	1	1.35	7092.031
C O Q 1	6	2	4	6	1	6	2.26	7091.996
C E R 1	2	2	0	1	1	0	1.35	7091.972
C E Q 1	7	2	6	7	1	6	2.53	7091.820
C E Q 1	6	2	5	6	1	5	2.31	7090.736
C O Q 1	5	2	3	5	1	5	1.99	7090.706
C E Q 1	22	1	22	22	0	22	2.40	7090.298
C O Q-1	27	0	27	27	1	27	0.90	7089.893
C E Q 1	5	2	4	5	1	4	2.03	7089.808
C O Q 1	4	2	2	4	1	4	1.66	7089.633
C E R 1	12	1	11	11	0	11	3.32	7089.601

C	E	Q	1	4	2	3	4	1	3	1.68	7089.035
C	O	Q	1	3	2	1	3	1	3	1.25	7088.775
C	E	Q	1	3	2	2	3	1	2	1.25	7088.416
C	E	R	-1	21	0	21	20	1	19	0.98	7087.810
C	E	Q	1	21	1	21	21	0	21	2.79	7086.635
C	E	R	1	11	1	10	10	0	10	3.43	7085.060
C	O	Q	-1	26	0	26	26	1	26	1.10	7084.344
C	E	Q	1	20	1	20	20	0	20	3.20	7083.155
C	E	R	-1	20	0	20	19	1	18	1.15	7082.669
C	O	P	1	14	2	13	15	1	15	0.84	7080.822
C	E	R	1	10	1	9	9	0	9	3.48	7080.736
C	E	Q	1	19	1	19	19	0	19	3.64	7079.854
C	O	P	1	13	2	12	14	1	14	0.90	7079.755
C	O	Q	-1	25	0	25	25	1	25	1.34	7078.985
C	O	P	1	12	2	11	13	1	13	0.94	7078.905
C	O	P	1	11	2	10	12	1	12	0.96	7078.271
C	O	P	1	7	2	6	8	1	8	0.83	7077.899
C	O	P	1	10	2	9	11	1	11	0.97	7077.854
C	O	P	1	8	2	7	9	1	9	0.90	7077.668
C	E	R	-1	19	0	19	18	1	17	1.33	7077.667
C	O	P	1	9	2	8	10	1	10	0.95	7077.653
C	E	Q	1	18	1	18	18	0	18	4.08	7076.733
C	E	R	1	9	1	8	8	0	8	3.47	7076.627
C	E	P	1	7	2	5	8	1	7	0.87	7075.770
C	E	P	1	8	2	6	9	1	8	0.95	7075.013
C	E	P	1	16	2	14	17	1	16	0.83	7074.888
C	E	P	1	9	2	7	10	1	9	1.01	7074.418
C	E	P	1	15	2	13	16	1	15	0.90	7074.311
C	E	P	1	10	2	8	11	1	10	1.04	7073.984
C	E	P	1	14	2	12	15	1	14	0.96	7073.907
C	O	Q	-1	24	0	24	24	1	24	1.60	7073.816
C	E	Q	1	17	1	17	17	0	17	4.53	7073.788
C	E	P	1	11	2	9	12	1	11	1.05	7073.715
C	E	P	1	13	2	11	14	1	13	1.00	7073.674
C	E	P	1	12	2	10	13	1	12	1.04	7073.611
C	E	R	-1	18	0	18	17	1	16	1.52	7072.805
C	E	R	1	8	1	7	7	0	7	3.39	7072.734
C	E	Q	1	16	1	16	16	0	16	4.97	7071.018
C	E	R	1	7	1	6	6	0	6	3.24	7069.054
C	O	Q	-1	23	0	23	23	1	23	1.90	7068.841
C	E	Q	1	15	1	15	15	0	15	5.37	7068.420
C	E	R	-1	17	0	17	16	1	15	1.72	7068.085
C	E	Q	1	14	1	14	14	0	14	5.74	7065.994
C	E	R	1	6	1	5	5	0	5	3.01	7065.588
C	O	Q	-1	22	0	22	22	1	22	2.23	7064.058
C	E	Q	1	13	1	13	13	0	13	6.05	7063.737
C	E	R	-1	16	0	16	15	1	14	1.91	7063.509
C	E	R	1	5	1	4	4	0	4	2.71	7062.335
C	E	Q	1	12	1	12	12	0	12	6.28	7061.649
C	E	Q	1	11	1	11	11	0	11	6.42	7059.726
C	O	Q	-1	21	0	21	21	1	21	2.59	7059.472
C	E	R	1	4	1	3	3	0	3	2.36	7059.294
C	E	R	-1	15	0	15	14	1	13	2.08	7059.076
C	E	Q	1	10	1	10	10	0	10	6.46	7057.969
C	E	R	1	3	1	2	2	0	2	1.94	7056.466

C	E	Q	1	9	1	9	9	0	9	6.39	7056.376
C	O	Q	-1	20	0	20	20	1	20	2.97	7055.082
C	E	Q	1	8	1	8	8	0	8	6.19	7054.945
C	E	R	-1	14	0	14	13	1	12	2.24	7054.788
C	E	R	1	2	1	1	1	0	1	1.49	7053.850
C	E	Q	1	7	1	7	7	0	7	5.86	7053.676
C	E	P	1	20	1	19	21	0	21	0.90	7053.334
C	E	Q	1	6	1	6	6	0	6	5.40	7052.567
C	E	Q	1	5	1	5	5	0	5	4.82	7051.619
C	E	R	1	1	1	0	0	0	0	1.00	7051.446
C	O	Q	-1	19	0	19	19	1	19	3.37	7050.890
C	E	P	1	19	1	18	20	0	20	1.06	7050.889
C	E	Q	1	4	1	4	4	0	4	4.12	7050.829
C	E	R	-1	13	0	13	12	1	11	2.37	7050.647
C	E	Q	1	3	1	3	3	0	3	3.32	7050.198
C	E	Q	1	2	1	2	2	0	2	2.43	7049.726
C	E	Q	1	1	1	1	1	0	1	1.49	7049.411
C	E	P	1	18	1	17	19	0	19	1.24	7048.679
C	O	Q	-1	18	0	18	18	1	18	3.77	7046.898
C	E	P	1	17	1	16	18	0	18	1.43	7046.702
C	E	R	-1	12	0	12	11	1	10	2.47	7046.653
C	E	P	1	16	1	15	17	0	17	1.62	7044.956
C	E	P	1	2	1	1	3	0	3	0.94	7043.951
C	E	P	1	15	1	14	16	0	16	1.81	7043.440
C	O	Q	-1	17	0	17	17	1	17	4.18	7043.107
C	E	R	-1	11	0	11	10	1	9	2.52	7042.808
C	E	P	1	3	1	2	4	0	4	1.35	7042.609
C	E	P	1	14	1	13	15	0	15	2.00	7042.152
C	E	P	1	4	1	3	5	0	5	1.71	7041.481
C	E	P	1	13	1	12	14	0	14	2.17	7041.090
C	E	P	1	5	1	4	6	0	6	2.00	7040.568
C	E	P	1	12	1	11	13	0	13	2.32	7040.252
C	E	P	1	6	1	5	7	0	7	2.23	7039.869
C	E	P	1	11	1	10	12	0	12	2.43	7039.638
C	O	Q	-1	16	0	16	16	1	16	4.58	7039.519
C	E	P	1	7	1	6	8	0	8	2.40	7039.387
C	E	P	1	10	1	9	11	0	11	2.50	7039.246
C	E	P	1	8	1	7	9	0	9	2.49	7039.121
C	E	R	-1	10	0	10	9	1	8	2.52	7039.112
C	E	P	1	9	1	8	10	0	10	2.53	7039.074
C	O	Q	-1	15	0	15	15	1	15	4.94	7036.134
C	E	R	-1	9	0	9	8	1	7	2.47	7035.566
C	O	Q	-1	14	0	14	14	1	14	5.27	7032.955
C	E	R	-1	8	0	8	7	1	6	2.35	7032.171
C	E	R	-1	16	1	15	15	2	13	0.82	7031.647
C	O	Q	-1	13	0	13	13	1	13	5.55	7029.982
C	E	R	-1	7	0	7	6	1	5	2.17	7028.927
C	O	Q	-1	12	0	12	12	1	12	5.76	7027.217
C	E	R	-1	15	1	14	14	2	12	0.86	7026.352
C	E	R	-1	6	0	6	5	1	4	1.93	7025.837
C	O	Q	-1	11	0	11	11	1	11	5.88	7024.660
C	E	R	-1	5	0	5	4	1	3	1.63	7022.899
C	O	Q	-1	10	0	10	10	1	10	5.91	7022.312
C	E	R	-1	14	1	13	13	2	11	0.89	7021.252
C	O	Q	-1	21	1	20	21	2	20	0.88	7020.589

C	O	Q-1	9	0	9	9	1	9	5.84	7020.175
C	E	R-1	4	0	4	3	1	2	1.27	7020.115
C	O	Q-1	8	0	8	8	1	8	5.65	7018.250
C	E	R-1	3	0	3	2	1	1	0.88	7017.485
C	O	Q-1	7	0	7	7	1	7	5.35	7016.536
C	E	R-1	13	1	12	12	2	10	0.91	7016.351
C	O	Q-1	20	1	19	20	2	19	1.02	7016.126
C	O	Q-1	6	0	6	6	1	6	4.92	7015.035
C	O	Q-1	5	0	5	5	1	5	4.39	7013.748
C	O	Q-1	4	0	4	4	1	4	3.75	7012.674
C	O	Q-1	19	1	18	19	2	18	1.16	7011.873
C	O	Q-1	3	0	3	3	1	3	3.02	7011.815
C	E	R-1	12	1	11	11	2	9	0.91	7011.651
C	O	Q-1	2	0	2	2	1	2	2.22	7011.170
C	O	Q-1	1	0	1	1	1	1	1.35	7010.740
C	E	P-1	0	0	0	1	1	0	0.90	7008.515
C	O	Q-1	18	1	17	18	2	17	1.31	7007.832
C	O	R-1	12	1	12	11	2	10	0.81	7007.489
C	E	R-1	11	1	10	10	2	8	0.89	7007.153
C	E	P-1	1	0	1	2	1	1	1.33	7006.661
C	E	P-1	2	0	2	3	1	2	1.72	7004.963
C	O	Q-1	17	1	16	17	2	16	1.46	7004.002
C	O	R-1	11	1	11	10	2	9	0.80	7003.615
C	E	P-1	3	0	3	4	1	3	2.06	7003.420
C	E	R-1	10	1	9	9	2	7	0.85	7002.859
C	E	P-1	4	0	4	5	1	4	2.35	7002.033
C	E	P-1	5	0	5	6	1	5	2.58	7000.802
C	E	Q-1	19	1	19	19	2	17	0.85	7000.749
C	E	P-1	20	0	20	21	1	20	0.93	7000.674
C	O	Q-1	16	1	15	16	2	15	1.61	7000.385
C	E	P-1	6	0	6	7	1	6	2.75	6999.725
C	E	P-1	19	0	19	20	1	19	1.10	6999.635
C	E	P-1	7	0	7	8	1	7	2.85	6998.804
C	E	P-1	18	0	18	19	1	18	1.29	6998.743
C	E	P-1	8	0	8	9	1	8	2.88	6998.037
C	E	P-1	17	0	17	18	1	17	1.49	6997.997
C	E	Q-1	18	1	18	18	2	16	0.99	6997.883
C	E	P-1	9	0	9	10	1	9	2.86	6997.424
C	E	P-1	16	0	16	17	1	16	1.70	6997.400
C	O	Q-1	15	1	14	15	2	14	1.75	6996.979
C	E	P-1	10	0	10	11	1	10	2.79	6996.964
C	E	P-1	15	0	15	16	1	15	1.92	6996.951
C	E	P-1	11	0	11	12	1	11	2.67	6996.658
C	E	P-1	14	0	14	15	1	14	2.13	6996.651
C	E	P-1	12	0	12	13	1	12	2.51	6996.504
C	E	P-1	13	0	13	14	1	13	2.33	6996.502
C	E	Q-1	17	1	17	17	2	15	1.14	6995.155
C	O	Q-1	14	1	13	14	2	13	1.88	6993.785
C	E	Q-1	16	1	16	16	2	14	1.29	6992.566
C	O	Q-1	13	1	12	13	2	12	1.98	6990.804
C	E	Q-1	15	1	15	15	2	13	1.44	6990.118
C	O	Q-1	12	1	11	12	2	11	2.07	6988.035
C	E	Q-1	14	1	14	14	2	12	1.59	6987.813
C	E	Q-1	13	1	13	13	2	11	1.72	6985.654
C	O	Q-1	11	1	10	11	2	10	2.12	6985.478

C	E	Q-1	12	1	12	12	2	10	1.83	6983.641
C	O	Q-1	10	1	9	10	2	9	2.13	6983.134
C	E	Q-1	11	1	11	11	2	9	1.91	6981.777
C	O	Q-1	9	1	8	9	2	8	2.11	6981.003
C	E	Q-1	10	1	10	10	2	8	1.96	6980.062
C	O	Q-1	8	1	7	8	2	7	2.04	6979.085
C	E	Q-1	9	1	9	9	2	7	1.96	6978.499
C	O	Q-1	7	1	6	7	2	6	1.92	6977.380
C	E	Q-1	8	1	8	8	2	6	1.92	6977.088
C	O	Q-1	6	1	5	6	2	5	1.75	6975.888
C	E	Q-1	7	1	7	7	2	5	1.84	6975.832
C	E	Q-1	6	1	6	6	2	4	1.69	6974.729
C	O	Q-1	5	1	4	5	2	4	1.53	6974.609
C	E	Q-1	5	1	5	5	2	3	1.50	6973.783
C	O	Q-1	4	1	3	4	2	3	1.27	6973.542
C	E	Q-1	4	1	4	4	2	2	1.25	6972.993
C	O	Q-1	3	1	2	3	2	2	0.95	6972.690
C	E	Q-1	3	1	3	3	2	1	0.94	6972.361
C	E	P-1	17	1	16	18	2	16	0.84	6967.852
C	E	P-1	1	1	0	2	2	0	1.00	6967.666
C	O	P-1	1	1	1	2	2	1	1.00	6967.611
C	E	P-1	16	1	15	17	2	15	0.93	6966.323
C	E	P-1	2	1	1	3	2	1	1.09	6966.113
C	O	P-1	2	1	2	3	2	2	1.08	6965.950
C	E	P-1	15	1	14	16	2	14	1.03	6964.988
C	E	P-1	3	1	2	4	2	2	1.18	6964.773
C	O	P-1	3	1	3	4	2	3	1.17	6964.447
C	E	P-1	14	1	13	15	2	13	1.12	6963.849
C	E	P-1	4	1	3	5	2	3	1.27	6963.646
C	O	P-1	4	1	4	5	2	4	1.25	6963.103
C	E	P-1	13	1	12	14	2	12	1.20	6962.909
C	E	P-1	5	1	4	6	2	4	1.34	6962.730
C	E	P-1	12	1	11	13	2	11	1.28	6962.169
C	E	P-1	6	1	5	7	2	5	1.39	6962.025
C	O	P-1	5	1	5	6	2	5	1.31	6961.919
C	E	P-1	11	1	10	12	2	10	1.34	6961.631
C	E	P-1	7	1	6	8	2	6	1.42	6961.530
C	E	P-1	10	1	9	11	2	9	1.39	6961.296
C	E	P-1	8	1	7	9	2	7	1.43	6961.245
C	E	P-1	9	1	8	10	2	8	1.42	6961.167
C	O	Q-1	17	2	15	17	3	15	0.84	6960.905
C	O	P-1	6	1	6	7	2	6	1.35	6960.893
C	E	Q-1	17	2	16	17	3	14	0.83	6960.456
C	O	P-1	7	1	7	8	2	7	1.36	6960.027
C	O	P-1	8	1	8	9	2	8	1.36	6959.321
C	O	P-1	15	1	15	16	2	15	0.87	6958.855
C	O	P-1	9	1	9	10	2	9	1.33	6958.774
C	O	P-1	14	1	14	15	2	14	0.96	6958.441
C	O	P-1	10	1	10	11	2	10	1.28	6958.387
C	O	P-1	13	1	13	14	2	13	1.06	6958.187
C	O	P-1	11	1	11	12	2	11	1.22	6958.160
C	O	P-1	12	1	12	13	2	12	1.14	6958.093
C	O	Q-1	16	2	14	16	3	14	0.93	6957.665
C	E	Q-1	16	2	15	16	3	13	0.93	6957.310
C	O	Q-1	15	2	13	15	3	13	1.02	6954.623

```
 C E Q-1  15   2  14   15   3  12   1.01              6954.347
 C O Q-1  14   2  12   14   3  12   1.09              6951.778
 C E Q-1  14   2  13   14   3  11   1.09              6951.566
 C O Q-1  13   2  11   13   3  11   1.16              6949.127
 C E Q-1  13   2  12   13   3  10   1.16              6948.969
 C O Q-1  12   2  10   12   3  10   1.21              6946.671
 C E Q-1  12   2  11   12   3   9   1.21              6946.555
 C O Q-1  11   2   9   11   3   9   1.24              6944.408
 C E Q-1  11   2  10   11   3   8   1.24              6944.325
 C O Q-1  10   2   8   10   3   8   1.25              6942.337
 C E Q-1  10   2   9   10   3   7   1.25              6942.280
 C O Q-1   9   2   7    9   3   7   1.23              6940.457
 C E Q-1   9   2   8    9   3   6   1.23              6940.419
 C O Q-1   8   2   6    8   3   6   1.18              6938.768
 C E Q-1   8   2   7    8   3   5   1.18              6938.744
 C O Q-1   7   2   5    7   3   5   1.10              6937.268
 C E Q-1   7   2   6    7   3   4   1.10              6937.254
 C O Q-1   6   2   4    6   3   4   0.98              6935.957
 C E Q-1   6   2   5    6   3   3   0.98              6935.949
 C O Q-1   5   2   3    5   3   3   0.82              6934.835
 C E Q-1   5   2   4    5   3   2   0.82              6934.831
 C E P-1   2   2   0    3   3   0   1.01              6926.661
 C O P-1   2   2   1    3   3   1   1.01              6926.661
 C E P-1   3   2   1    4   3   1   1.03              6925.244
 C O P-1   3   2   2    4   3   2   1.03              6925.243
 C E P-1   4   2   2    5   3   2   1.04              6924.014
 C O P-1   4   2   3    5   3   3   1.04              6924.013
 C E P-1   5   2   3    6   3   3   1.06              6922.973
 C O P-1   5   2   4    6   3   4   1.06              6922.969
 C E P-1   6   2   4    7   3   4   1.06              6922.119
 C O P-1   6   2   5    7   3   5   1.06              6922.111
 C E P-1   7   2   5    8   3   5   1.05              6921.455
 C O P-1   7   2   6    8   3   6   1.05              6921.440
 C E P-1  12   2  10   13   3  10   0.84              6920.991
 C E P-1   8   2   6    9   3   6   1.03              6920.980
 C O P-1   8   2   7    9   3   7   1.03              6920.956
 C O P-1  12   2  11   13   3  11   0.84              6920.878
 C E P-1  11   2   9   12   3   9   0.90              6920.700
 C E P-1   9   2   7   10   3   7   1.00              6920.695
 C O P-1   9   2   8   10   3   8   1.00              6920.657
 C O P-1  11   2  10   12   3  10   0.90              6920.619
 C E P-1  10   2   8   11   3   8   0.96              6920.602
 C O P-1  10   2   9   11   3   9   0.96              6920.545
Std. Dev. =  0.00000 for       0 lines with |Obs-Calc| less than
0.10000
Calculated lines =     487 Observed lines =       0
Temporary intensity minimum:  0.800
Output in <filename>.SUB
Output in <filename>.TMP
Phase II Completed

Asyrotwin Phase VII

HO2-electronic
```

```
Scale: Linear
Line shape: Lorentzian
Spectrum divided into   1000 intervals from   8000.000 to   6000.000
Half width:  0.050
The linear intensity output has been scaled from 0.0 to 1.0
Output in <filename>.PLT
Phase VII Completed
```